Supporting Information

Covalent Organic Framework with Frustrated Bonding Network for Enhanced Carbon Dioxide Storage

Qiang Gao[†,‡], Xing Li[‡], Guo-Hong Ning[‡], Hai-Sen Xu[‡], Cuibo Liu[†,‡], Bingbing Tian[†,‡], Wei Tang[‖], Kian Ping Loh[*,†,‡]

† SZU-NUS Collaborative Innovation Center for Optoelectronic Science & Technology, Key Laboratory of Optoelectronic Devices and Systems of Ministry of Education and Guangdong Province, College of Optoelectronic Engineering, Shenzhen University, Shenzhen 518060, China
‡ Department of Chemistry, Centre for Advanced 2D Materials (CA2DM), National University of Singapore, 3 Science Drive 3, Singapore 117543, Singapore
‖ Institute of Materials Research and Engineering, A*STAR, 2 Fusionopolis Way, Innovis, Singapore 138634, Singapore.

*Corresponding author: Professor Kian Ping Loh (e-mail: chmlohkp@nus.edu.sg)

I. General Procedure

All starting materials and solvents are commercially available (purchased from *Sigma Aldrich* or *TCI*) and were used as received unless specifically mentioned.

Thermogravimetric analysis (TGA): TGA characterization was performed on a TGA 500 thermogravimetric analyzer by heating the samples at 5 ºC min^{-1} to 800 ºC in a nitrogen atmosphere.

Fourier transform infrared (FT-IR): Fourier transform infrared spectra were recorded as KBr-pellet on a Bruker OPUS/IR PS15 spectrometer.

Scanning Electron Microscopy (SEM) and Transmission Electron Microscopy (TEM): SEM imaging of the COF pristine materials were performed using a JEOL JSM-6701F Field-Emission. TEM imaging of COF pristine materials was performed on an FEI Titan 80-300 S/TEM (Scanning /Transmission Electron Microscope) operated at 200 kV.

Powder X-ray Diffraction (PXRD) measurements: PXRD studies were performed on collected on Bruker D8 Focus Powder X-ray diffractometer using Cu Kα radiation (40 kV, 40 mA) with a step size of 0.032 º/min over 2θ range of 2º - 35º at room temperature.

Gas Sorption measurements: Gas sorption analyses were performed by using Quantachrome Instruments Autosorb-iQ with extra-high pure gases. The samples were activated and outgassed at 120 ºC for 8 h before the measurements. The Brunauer-Emmett-Teller (BET) surface area and total pore volume were calculated from the N_2 sorption isotherms at 77 K, and the pore size distribution was calculated based on the N_2 sorption isotherm by using DFT models in the Quantachrome ASiQwin 5.0 software package. The isosteric heats of adsorption (Q_{st}) for CO_2 was calculated using Clausius-Clapeyron equation and determined by using CO_2 (273K and 298 K) adsorption isotherms, respectively.

$$Q_{\mathrm{st}} = \mathrm{RT}^2 \left(\frac{\partial \ln P}{\partial T}\right)_q \text{ (Clausius-Clapeyron equation)}$$

Nuclear Magnetic Resonance spectroscopy (NMR):^{1}H and ^{13}C NMR spectra were recorded on a Bruker AVIII (400MHz) NMR spectrometer. Chemical shifts were reported in parts per million (ppm), and the residual solvent peak was used as an internal reference: proton (chloroform δ 7.26), carbon (chloroform δ 77.0) was used as a reference. Data are reported as follows: chemical shift, multiplicity (s = singlet, d = doublet), coupling constants (Hz) and integration. Solid-state ^{13}C cross-polarization/magic angle spinning nuclear magnetic resonance (CP/MAS NMR): Solid-state CP/MAS NMR measurement was conducted using a JEOL ECA400 solid-state NMR spectrometer, 4mm CPMAS probe, 100 MHz NMR spectrometer with spin rate as 8000 MHz.

High resolution mass spectra (HRMS): HRMS was obtained on Bruker micrOTOF-Q II coupled with a Dionex Ultimate 3000 RSLC system and Kd Science Syringe pump infusion system.

Structural Modeling Method: Molecular modeling and Pawley refinement were carried out using Reflex, a software package for crystal determination from Powder XRD pattern, implemented in

BIOVIA Materials Studio modeling version, 2016 (Dassault System). The unit cells for TPE-COFs were established, the lattice model was geometry optimized using the MS Forcite molecular dynamics module (ultra-fine, Universal force fields, Ewald summations). Finally, Pawley refinement was performed to optimize the lattice parameters until the $_{W}R_{P}$ value converges. The pseudo-Voigt profile function was used for whole profile fitting and Berrar–Baldinozzi function was used for asymmetry correction during the refinement processes.

II. Synthesis of TPE Building Units and Model Compounds (1-4):

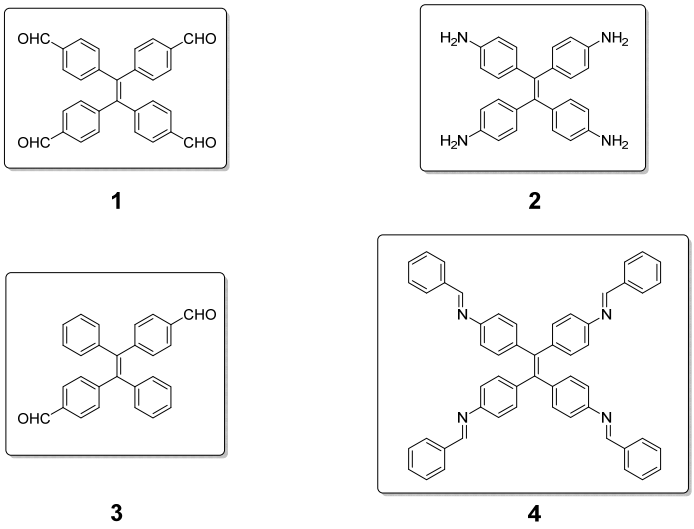

Figure S1. Chemical structures of monomer TPE-4CHO (**1**), TPE-4NH_2 (**2**), *trans*-TPE-2CHO (**3**) and TPE model compound TPE-M (**4**).

a) 1, 3, 6, 8-tetrakis(4-aminophenyl)ethane (**2**)[1] and TPE model compound (TPE-M, **4**)[2] were synthesized via the methods reported, respectively.

b) 1, 1, 2, 2-tetrakis(4-formylphenyl)ethane (TPE-4CHO, **1**) were synthesized in accordance to literature reported method with slight modifications[3]:

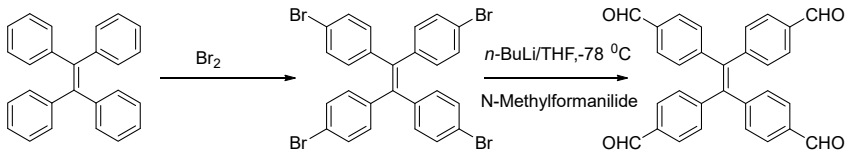

Step I. To an ice-water bath solution of 1, 1, 2, 2-Tetraphenylethylene (TPE, **5**, 6.64 g, 20 mmol) in 40 mL glacial acetic acid, Bromine (8.3 mL, 160 mmol) was added dropwise via a pressure equalizing dropping funnel in 15 minutes, under Argon atmosphere. After further adding 30 mL dichloromethane (DCM), the solution was heated to 50 ºC for 30 minutes. The reaction mixture was then carefully poured into 200 mL ice water, the resulted precipitate was filtered and washed with 50 mL water and 50 mL ethanol, three times respectively. After dried at 100 ºC under vacuum overnight, the obtained product tetra(4-bromophenyl)ethylene (**6**) was used directly for next step without further purification.

Step II. Tetra(4-bromophenyl)ethylene (**6**, 6.48 g, 10 mmol) was added to a 1000 mL two-necked round-bottom flask, the flask was evacuated and flushed with Argon for three times. Anhydrous tetrahydrofuran (THF, 250 mL) was then added to the flask with syringe. After stirring for 15 minutes, the reaction mixture was cooled to -78 ºC, then *n*-BuLi (25 mL, 2 M in cyclohexane, 50 mmol) was added dropwise via syringe in around 30 minutes. After further stirring at -78 ºC for 3 hours, a solution of N-methylformanilide (10 mL, 80 mmol) in 100 mL THF was added dropwise in 30 minutes. The reaction mixture was further stirred at -78 ºC for another 2 hours, then warmed to room temperature and stirred at room temperature overnight. The reaction was then quenched by dilute HCl solution, most of the THF was removed by rotary

evaporator. The residue was extracted with 200 mL DCM three times. After dried over anhydrous Na_2SO_4 and evaporating the solvent of combined organic layers, the crude product was purified by silica column chromatography using *n*-Hexane/ethyl acetate (10:1) as eluent. Light yellow solid of 1, 1, 2, 2-tetrakis(4-formylphenyl)ethane (TPE-4CHO, **1**) was obtained in 60% yield (2.67 g).

^{1}H NMR (400 MHz, Chloroform-*d*) δ 9.94 (s, 4H), 7.69 (d, *J* = 1.8 Hz, 4H), 7.67 (d, *J* = 1.8 Hz, 4H), 7.19 (d, *J* = 1.8 Hz, 4H), 7.18 (d, *J* = 1.7 Hz, 4H).

^{13}C NMR (100 MHz, Chloroform-*d*) δ 191.50, 148.02, 142.34, 135.51, 131.89, 129.74.

HR-MS (APCI) m/z Calcd. for [$C_{30}H_{21}O_4$] 445.1435; Found: 445.1434.

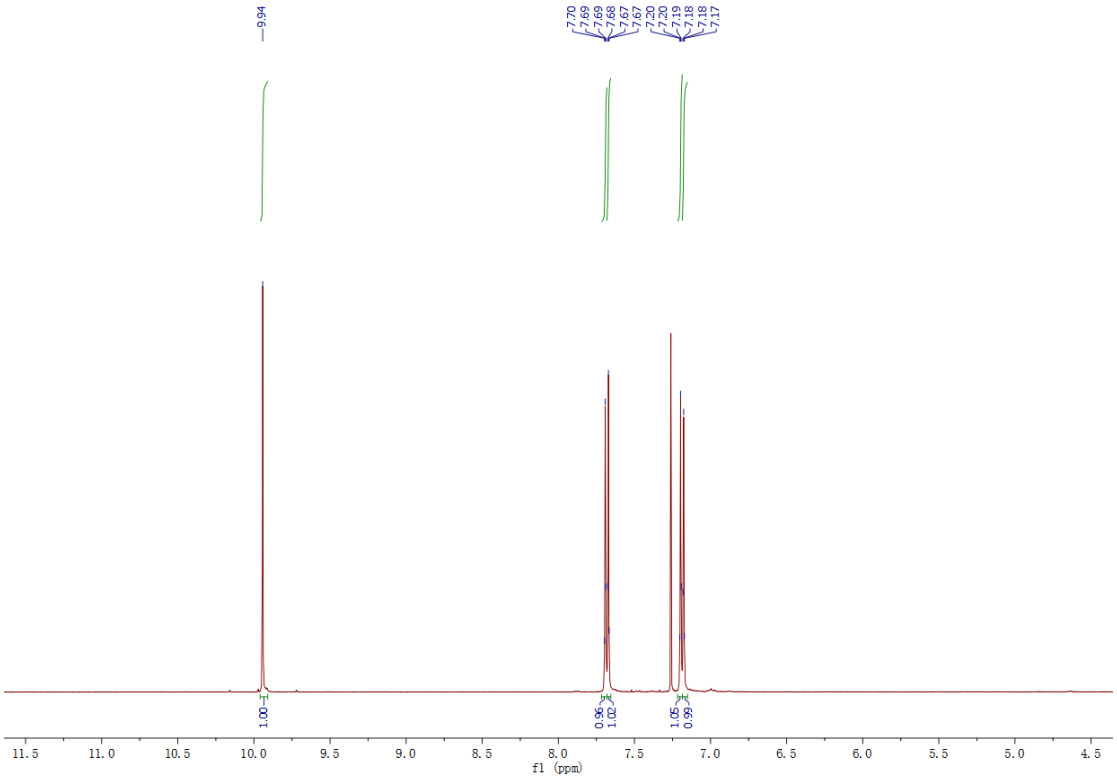

Figure S2. ^{1}H NMR spectrum of 1, 1, 2, 2-tetrakis(4-formylphenyl)ethane (**1**).

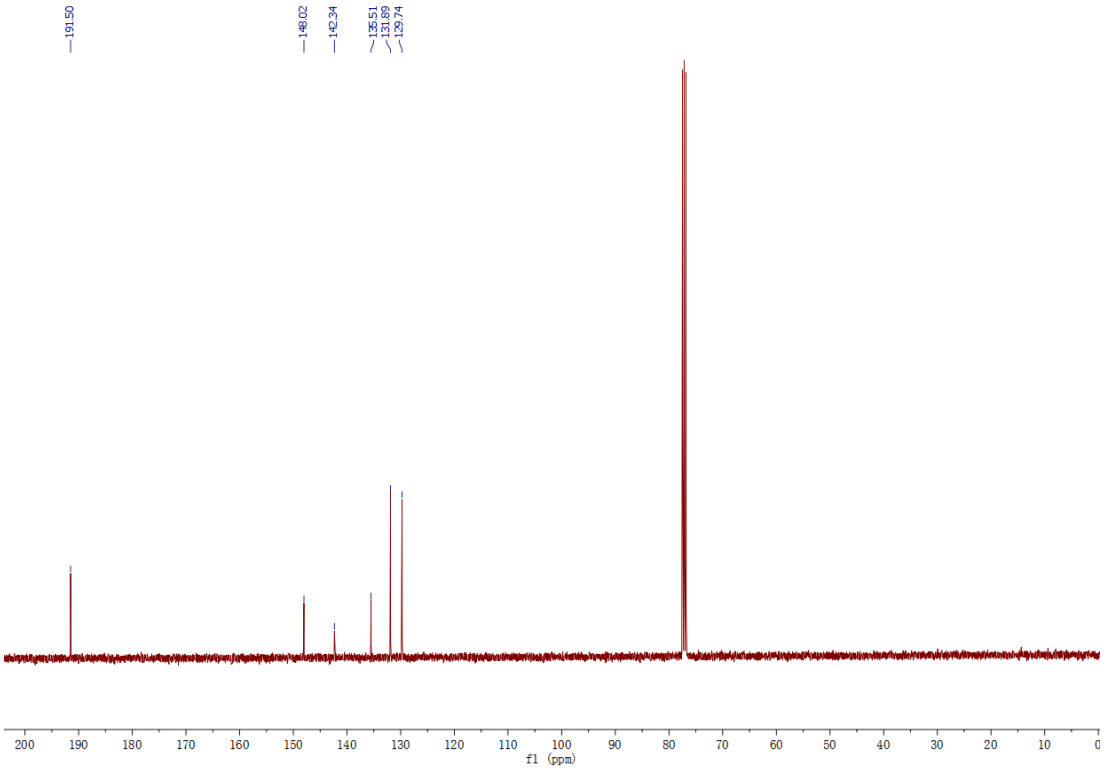

Figure S3. ^{13}C NMR spectrum of 1, 1, 2, 2-tetrakis(4-formylphenyl)ethane (**1**).

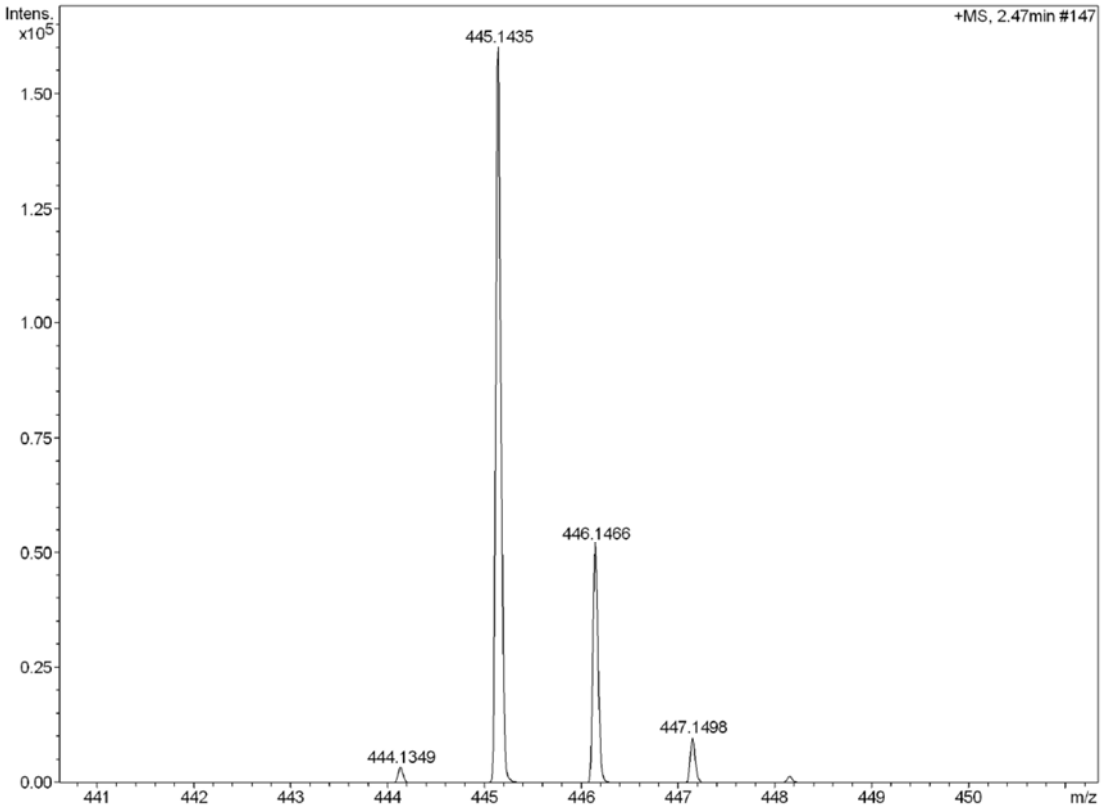

Figure S4. HR-MS of 1, 1, 2, 2-tetrakis(4-formylphenyl)ethane (**1**).

c) (*E*)-4,4'-(1,2-diphenylethene-1,2-diyl)dibenzaldehyde (*trans*-TPE-2CHO, **3**) were synthesized in accordance to literature reported method with slight modifications[3]:

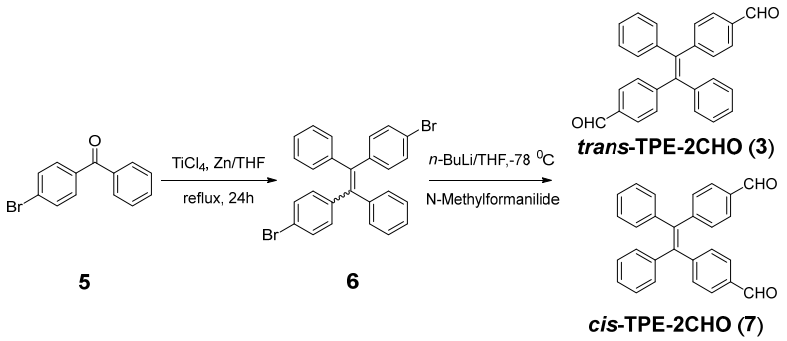

Step I. 1,2-bis(4-bromophenyl)-1,2-diphenylethene (**6**): The three-necked 500 mL flask, placed with 4-bromobenzophenone (5) (10.0 g, 38.3 mmol) with zinc powder (7.52 g, 114.9 mmol), was evacuated under vacuum and flushed with dry Argon three times. After adding tetrahydrofuran (anhydrous, 150 mL) into the flask, the mixture was cooled down to 0 °C. $TiCl_4$ (10.89 g, 6.4 mL, 57.4 mmol) was added dropwise in 30 minutes, then the mixture was refluxed for 24 hours. After cooled to room temperature, the mixture was filtered and washed with dichloromethane (DCM). The filtrate was poured into dilute HCl solution (100 mL), and extracted by DCM three times. The collected organic phase was dried over Na_2SO_4, evaporated with reduced pressure. The crude product was purified by silica column chromatography using n-hexane as eluent. 1, 2-bis(4-bromophenyl)-1,2-diphenylethene (**6**) was obtained as white solid (8.2 g, 87% yield)

Step II. (*E*)-4, 4'-(1, 2-diphenylethene-1, 2-diyl)dibenzaldehyde (**3**): 1, 2-bis(4-bromophenyl)-1,2-diphenylethene (**6**, 4.0 g, 8.16 mmol) was added into a dried, three-necked 500 mL flask. The flask was evacuated under vacuum and flushed with dry Argon three times. Then tetrahydrofuran (anhydrous, 250 mL) was injected into the flask. After the reaction system was cooled to -78 °C, *n*-BuLi (12.2 mL, 1.6 M, 19.6 mmol) was added dropwise, the resulting mixture was stirred at -78 °C for 3 hours. N-methylformanilide (4.0 mL, 32.6 mmol, dissolved in 40 mL THF) was added dropwise with vigorous stirring. The mixture was stirred at -78 °C for 2 hours and warmed up to room temperature for 12 hours. The reaction was then quenched by dilute HCl solution. The mixture was extracted with DCM and the organic layer was combined and dried over Na_2SO_4.The crude product was purified by silica column chromatography using hexane /ethyl acetate (EA) mixture (20/1 by volume) as eluent, carefully. The *cis* and *trans* products can be separated. Light yellow solid of (*E*)-4,4'-(1,2-diphenylethene-1,2-diyl)dibenzaldehyde (**3**) was obtained in 39% yield (1.24 g).

^{1}H NMR (500 MHz, Chloroform-*d*) δ 9.91 (s, 1H), 7.66 – 7.60 (m, 2H), 7.23 – 7.18 (m, 2H), 7.18 – 7.11 (m, 3H), 7.03 – 6.97 (m, 2H).

^{13}C NMR (126 MHz, Chloroform-*d*) δ 191.90, 149.84, 142.29, 141.88, 134.75, 131.98, 131.34, 129.33, 128.34, 127.61.

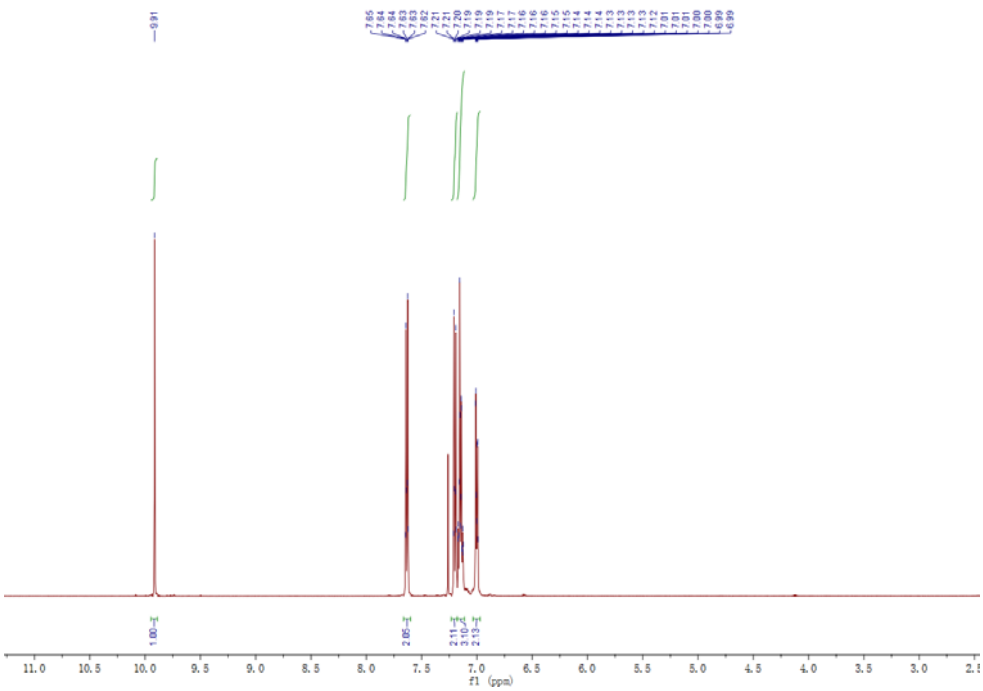

Figure S5. ^{1}H NMR spectrum of (*E*)-4, 4'-(1, 2-diphenylethene-1, 2-diyl)dibenzaldehyde (**3**).

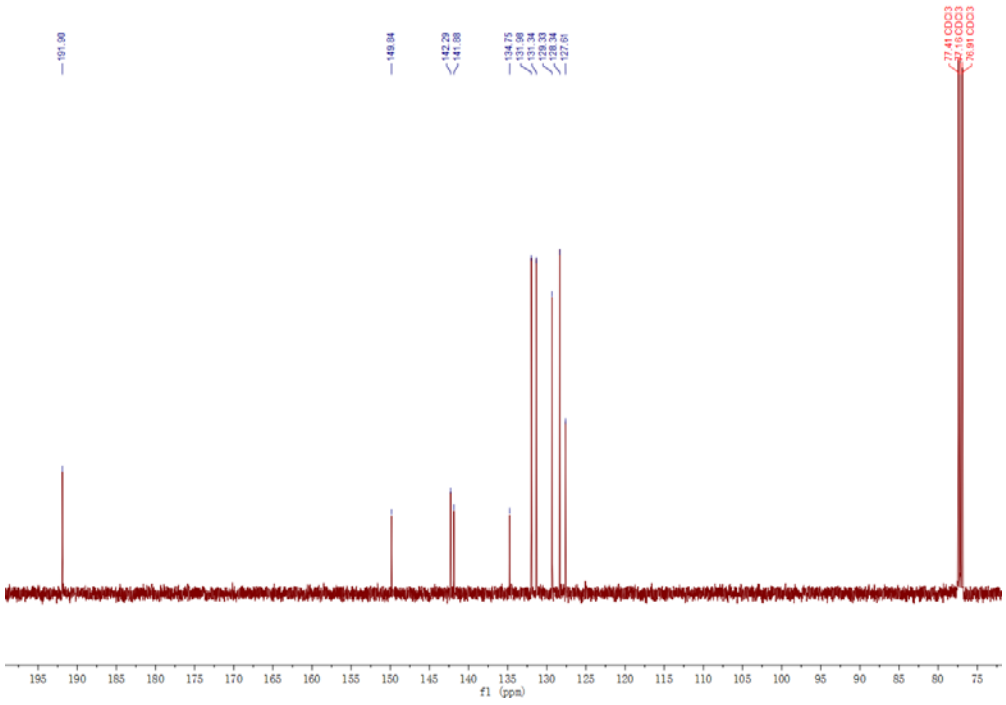

Figure S6. ^{13}C NMR spectrum of (*E*)-4, 4'-(1, 2-diphenylethene-1, 2-diyl)dibenzaldehyde (**3**).

Single crystal structure of (*E*)-4,4'-(1,2-diphenylethene-1,2-diyl)dibenzaldehyde (*trans*-TPE-2CHO, 3): CCDC 1585213

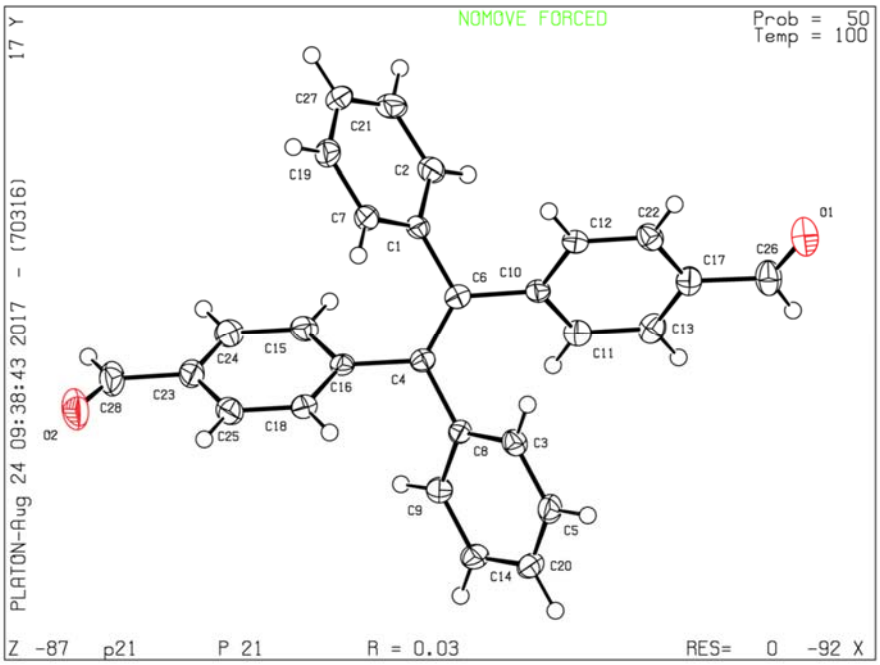

Table S1. Crystallographic data and structure refinement summary for compound **3**.

Formula	$C_{28}H_{20}O_2$
Mr	388.44
Temperature (K)	100
Wavelength (Å)	1.54178
Crystal system	Monoclinic
Space group	P_{21}
a, b, c/Å	a=9.9059(17), b=9.0034(16), c=12.075(2)
α, β, γ/°	α=90, β=105.605(8), γ=90
V/ Å^3	1037.2(3)
Z	2
D_{calc} (g·cm^{-3})	1.244
Crystal size (mm)	0.2× 0.16×0.1
Theta range (deg)	3.801 to 72.496
Reflections unique/collected	4105/9437
R_{int}	0.0252
Goodness-of-fit on F^2	1.001

III. Detailed Synthesis of TPE-COFs (TPE-COF-I, TPE-COF-II and TPE-COF-III)

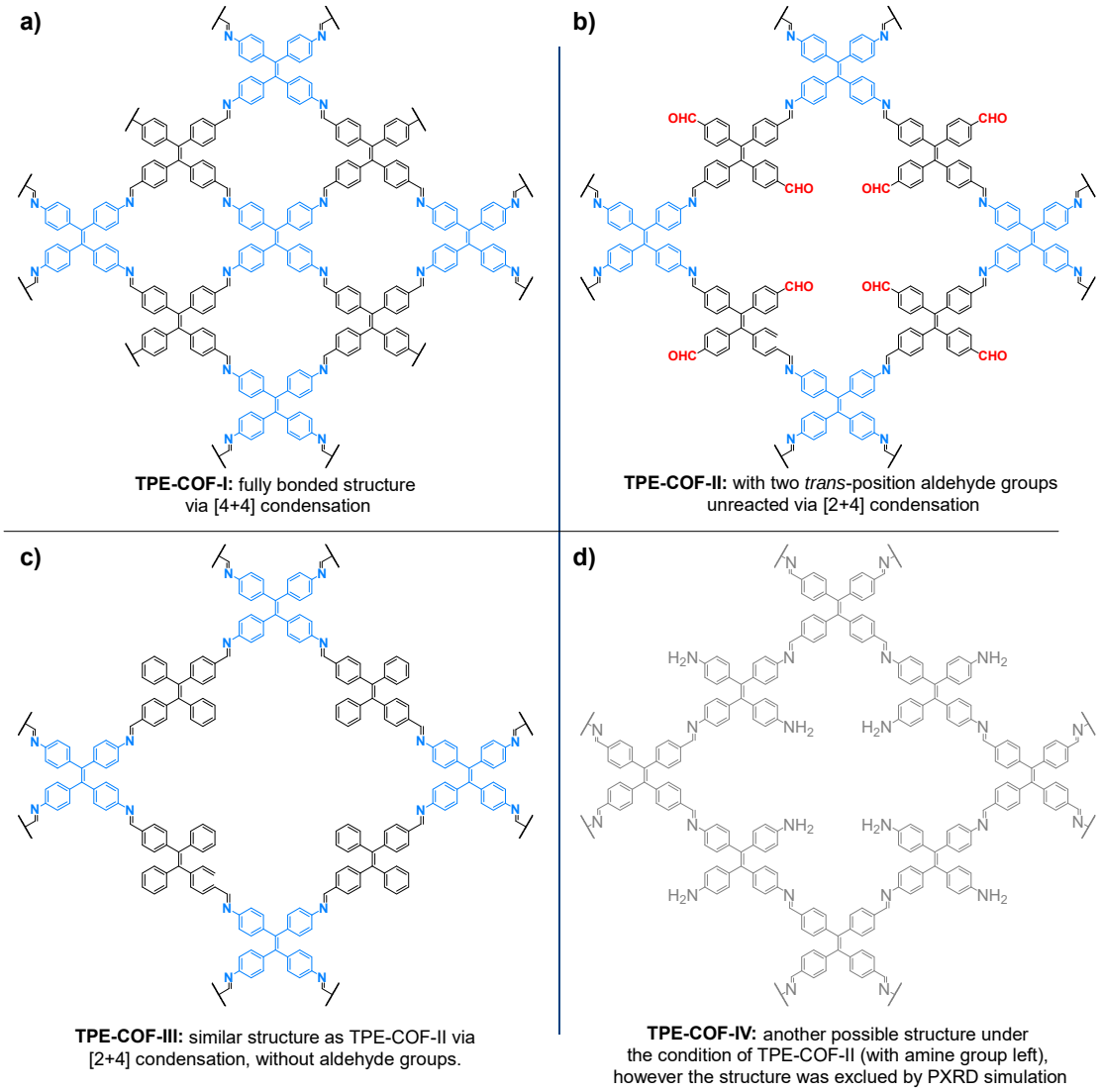

TPE-COF-I: fully bonded structure via [4+4] condensation

TPE-COF-II: with two *trans*-position aldehyde groups unreacted via [2+4] condensation

TPE-COF-III: similar structure as TPE-COF-II via [2+4] condensation, without aldehyde groups.

TPE-COF-IV: another possible structure under the condition of TPE-COF-II (with amine group left), however the structure was exclued by PXRD simulation

Figure S7. Schematic representation structural difference among (a) TPE-COF-I, (b) TPE-COF-II, (c) TPE-COF-III and (d) TPE-COF-IV. Compared with TPE-COF-III, the red-marked aldehyde indicated the two *trans*-position unreacted groups existed in TPE-COF-II.

a) Optimized Synthesize Methods and crystallization kinetics of **TPE-COF-I**

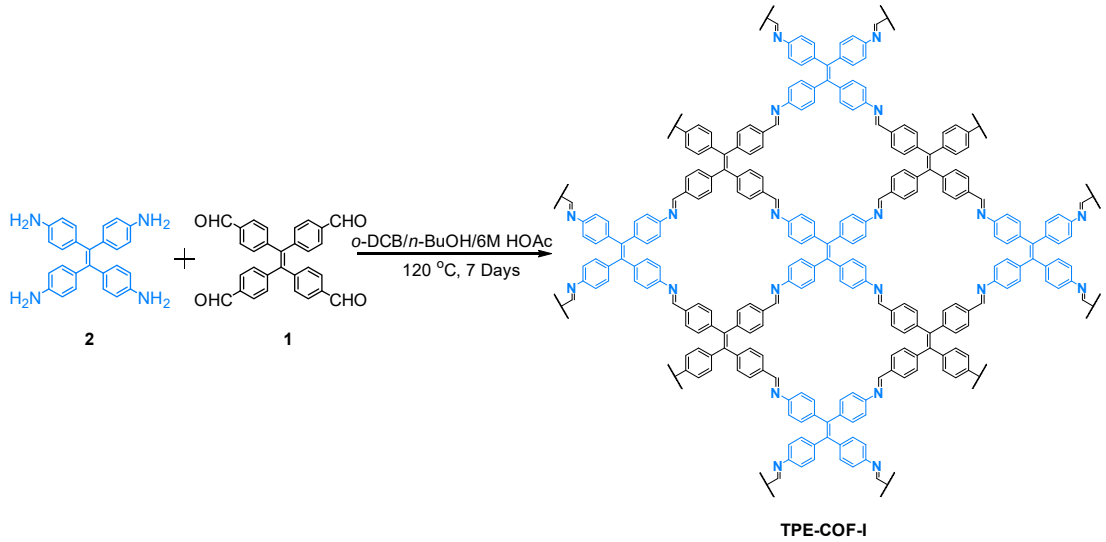

TPE-4NH$_2$ (**2**, 19.6 mg, 0.05mmol) and TPE-4CHO (**1**, 22.2 mg, 0.05 mmol) were placed in a 10 mL Synthware^{TM} schlenk storage tube, then the mixture was dissolved in solvent (3 mL o-dichlorobenzene/n-butanol, 1:1 V/V). Then, aqueous 0.2 mL 6M HOAc was added, and the mixture was degassed by three freeze-pump-thaw cycles. Finally, the tube was sealed via the screw cap, heated at 120 ℃ in an oven, and left undisturbed for 7 days. To obtained precipitate was then immersed and washed in THF three times. Then the powder was dried at 120 ℃ under vacuum for 24 h. A yellow powder was obtained in 87% isolation yield. Anal. Calcd. for $[C_{56}H_{36}N_4]_n$: C, 87.47; H, 5.24; N, 7.32. Found: C, 83.50; H, 6.11; N, 7.07.

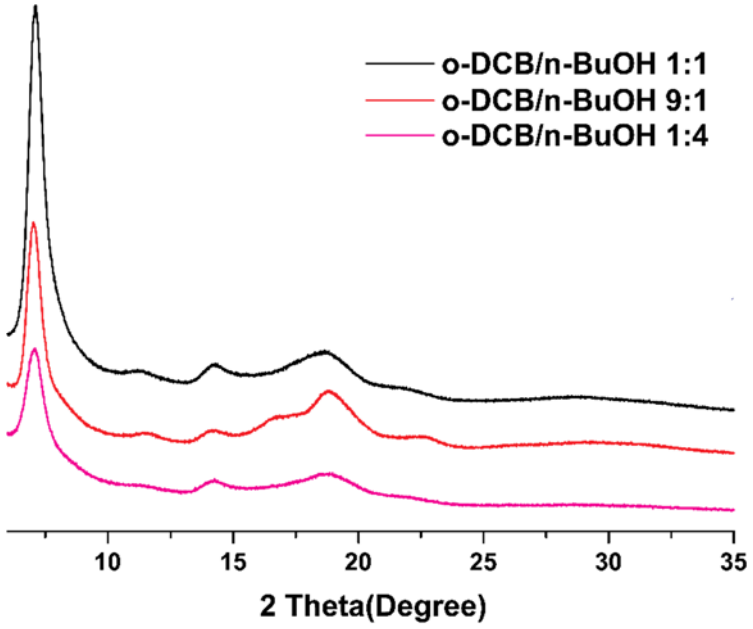

Figure S8. Experimental Powder XRD patterns of TPE-COF-I materials under different *o*-DCB/*n*-BuOH ratios (from 9:1 to 1:4), which indicating the best crystallinity was obtained under the ratio of 1:1.

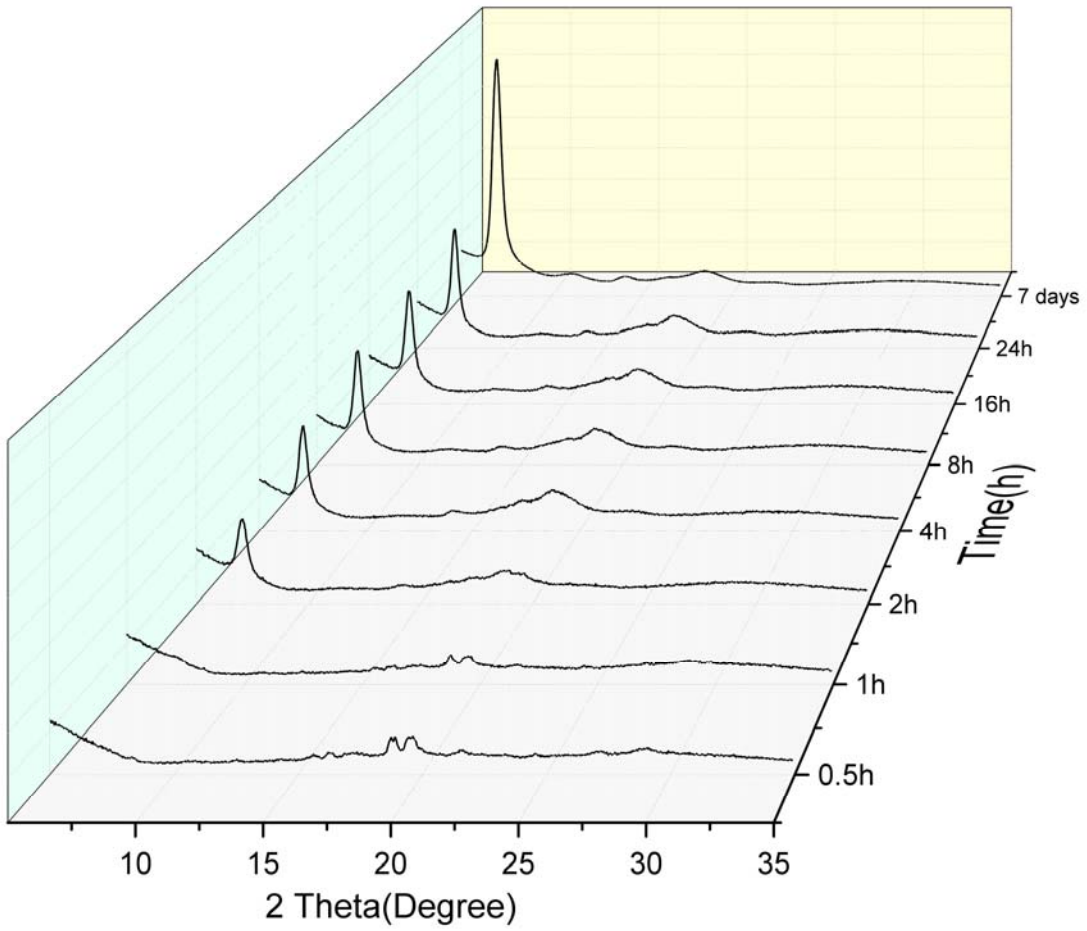

Figure S9. Experimental PXRD patterns of TPE-COF-I under different solvothermal times ranging from 0.5 h to 7 days. Crystallization kinetics of the TPE-COF-I: Amorphous precipitate from the initial reaction solution slowly begins to crystallize to form the ordered COF structure one hour later, meanwhile the reflections from fragments (around 20°) began to decrease. After 2 hours-reaction, the increasing intensity of reflections at 7.1°, 11.3°, 14.2°, 18.6° indicates that the degree of crystallinity continues to improve with time.

b) Optimized Synthesize Methods and crystallization kinetics of **TPE-COF-II:**

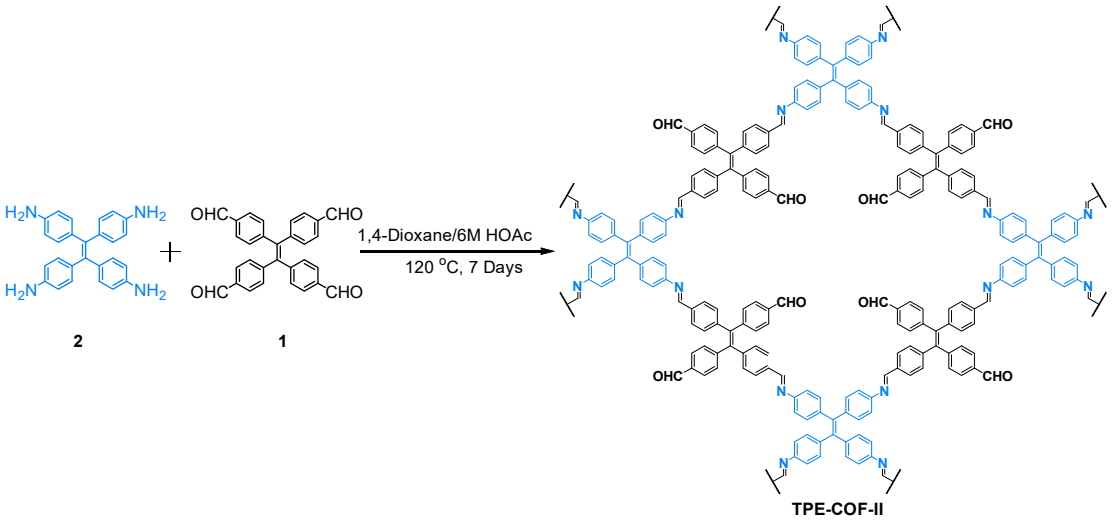

TPE-COF-II: TPE-4NH$_2$ (**2**, 9.8 mg, 0.025mmol) and TPE-4CHO (**1**, 22.2 mg, 0.05 mmol) were placed in a 10 mL Synthware^{TM} schlenk storage tube, then the mixture was dissolved in solvent (3 mL 1, 4-dioxane). Then, aqueous 0.2 mL 6M HOAc was added, and the mixture was degassed by three freeze-pump-thaw cycles. Finally, the tube was sealed via the screw cap, heated at 120 ℃ in an oven, and left undisturbed for 7 days. To obtained precipitate was then immersed and washed in THF three times. Then the powder was dried at 120 ℃ under vacuum for 24 h. A yellow powder was obtained in 93% isolation yield. Anal. Calcd. for $[C_{86}H_{56}N_4O_4]_n$: C, 85.41; H, 4.67; N, 4.63. Found: C, 81.09; H, 5.80; N, 6.34.

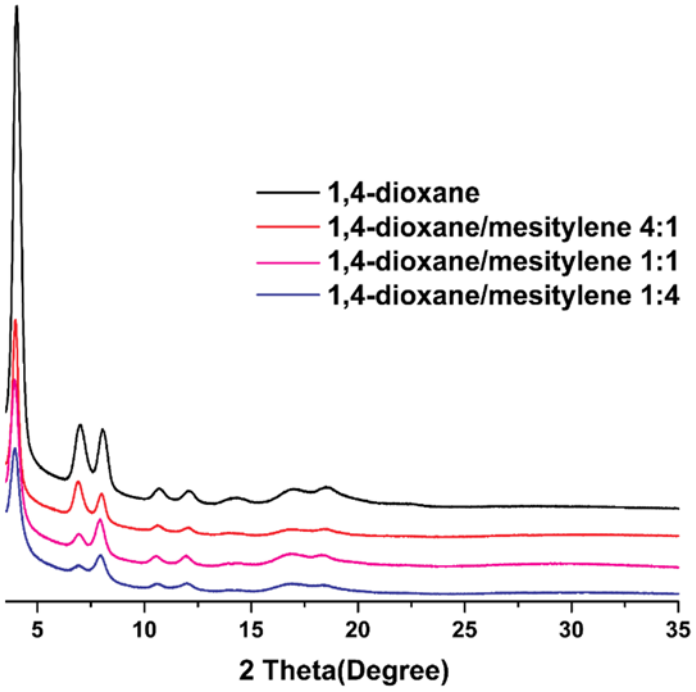

Figure S10. Experimental Powder XRD patterns of TPE-COF-II under different 1, 4-dioxane / mesitylene ratios (from 4:1 to 1:4), which indicating the best crystallinity was obtained under the pure 1, 4-dioxane.

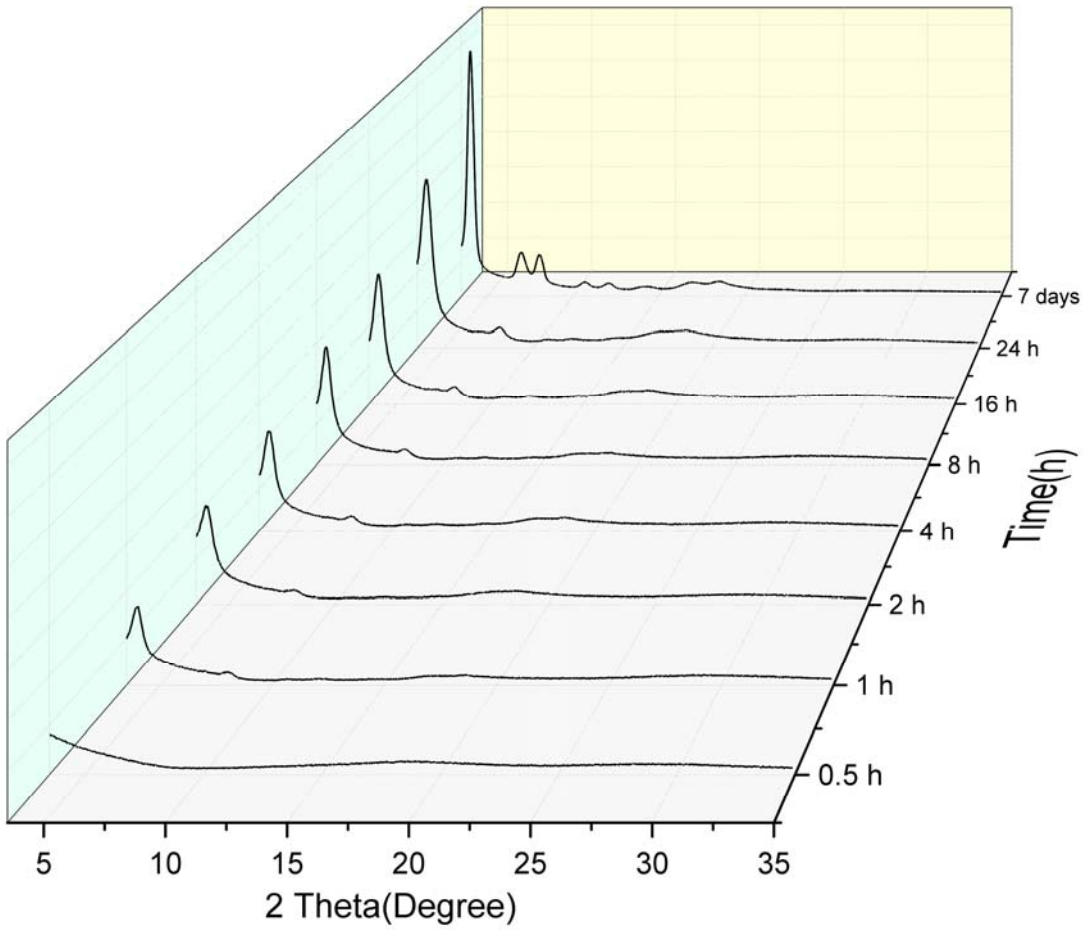

Figure S11. Experimental PXRD patterns of TPE-COF-II under different solvothermal times ranging from 0.5 h to 7 days. Crystallization kinetics of the TPE-COF-II: Amorphous precipitate from the initial reaction solution slowly begins to crystallize to form the ordered COF structure half an hour. After one hour-reaction, the increasing intensity of reflections at 4.0°, 7.0°, 8.0°, 11.7°, 12.1°, 14.3°, 16.9° and 18.6° indicates that the degree of crystallinity continues to improve with time.

c) Synthesis of TPE-COF-III:

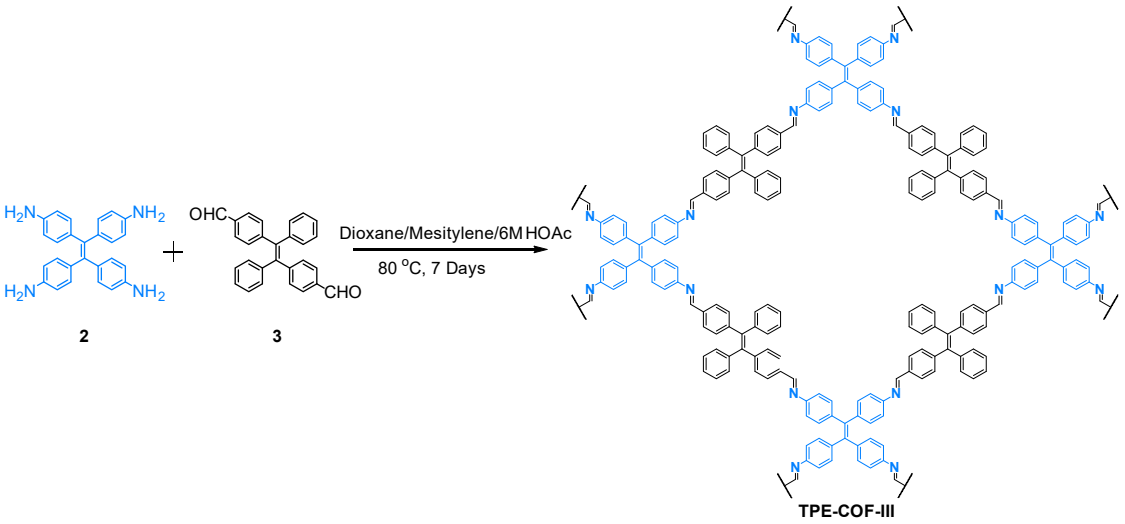

TPE-COF-III: TPE-4NH_2 (**1**, 19.6 mg, 0.05 mmol) and *trans*-TPE-2CHO (**3**, 38.8 mg, 0.1 mmol) were were placed in a 10 mL Synthware^{TM} schlenk storage tube, then the mixture was dissolved in solvent (3 mL, 1,4-dioxane /mesitylene, 1:1 V/V). Then, aqueous 0.2 mL 6M HOAc was added, and the mixture was degassed by three freeze-pump-thaw cycles. Finally, the tube was sealed via the screw cap, heated at 80 °C in an oven, and left undisturbed for 7 days. To obtained precipitate was then immersed and washed in THF three times. Then the powder was dried at 120 °C under vacuum for 24 h. A yellow powder was obtained in 83% isolation yield. Anal. Calcd. for $[C_{82}H_{56}N_4]_n$: C, 89.75; H, 5.14; N, 5.11. Found: C, 86.78; H, 5.32; N, 5.15.

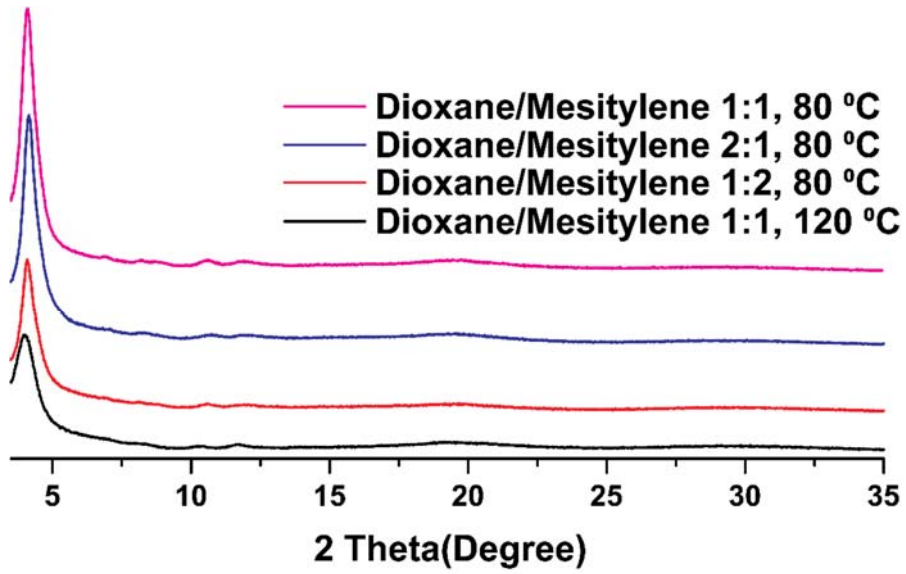

Figure S12. Powder XRD pattern of COF material TPE-COF-III under different 1, 4-dioxane / mesitylene ratios and different temperatures (from 2:1 to 1:2), which indicating the best crystallinity was obtained under the under the ratio of 1:1, 80 °C. (Note: TPE-COF-III was obtained with very low yield under 120 °C, 17% yield, due to the *trans*-TPE-2CHO)

d) The Comparison for Experimental PXRD patterns of TPE-COFs:

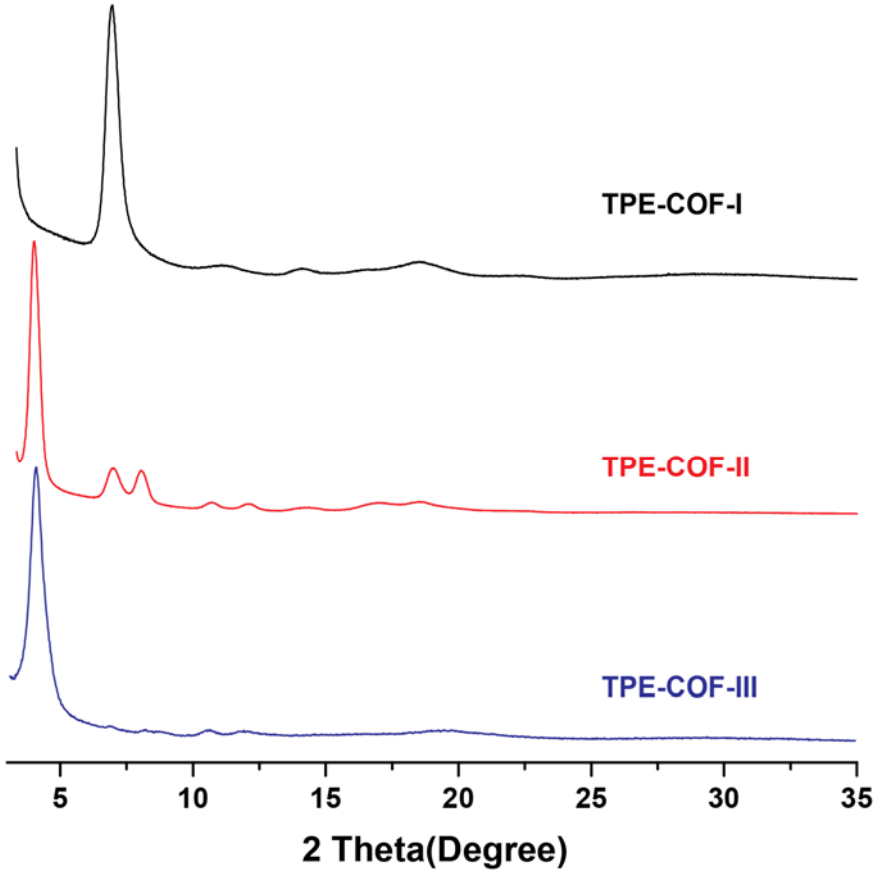

Figure S13. Powder XRD patterns of TPE-COFs, indicating that obviously different structures between TPE-COF-I and TPE-COF-II, and the similar structures between TPE-COF-II and TPE-COF-III.

IV. Solid-state ^{13}C CP/MAS NMR spectra of TPE-COFs

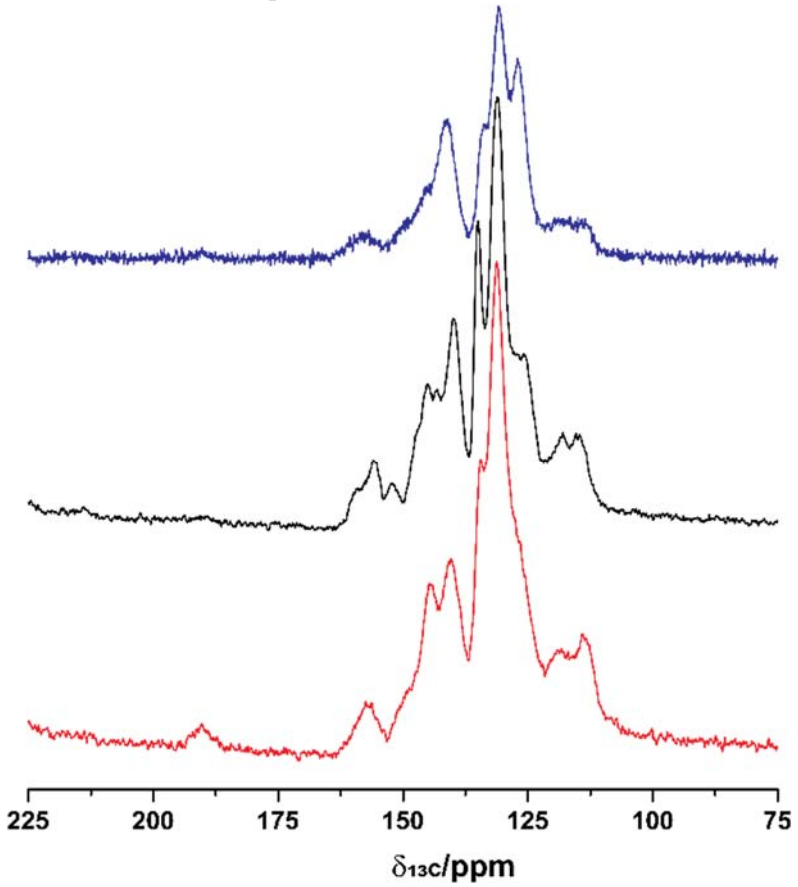

Figure S14. Solid-state ^{13}C CP/MAS NMR spectra of TPE-COF-I (black), TPE-COF-II (red), TPE-COF-III (blue).

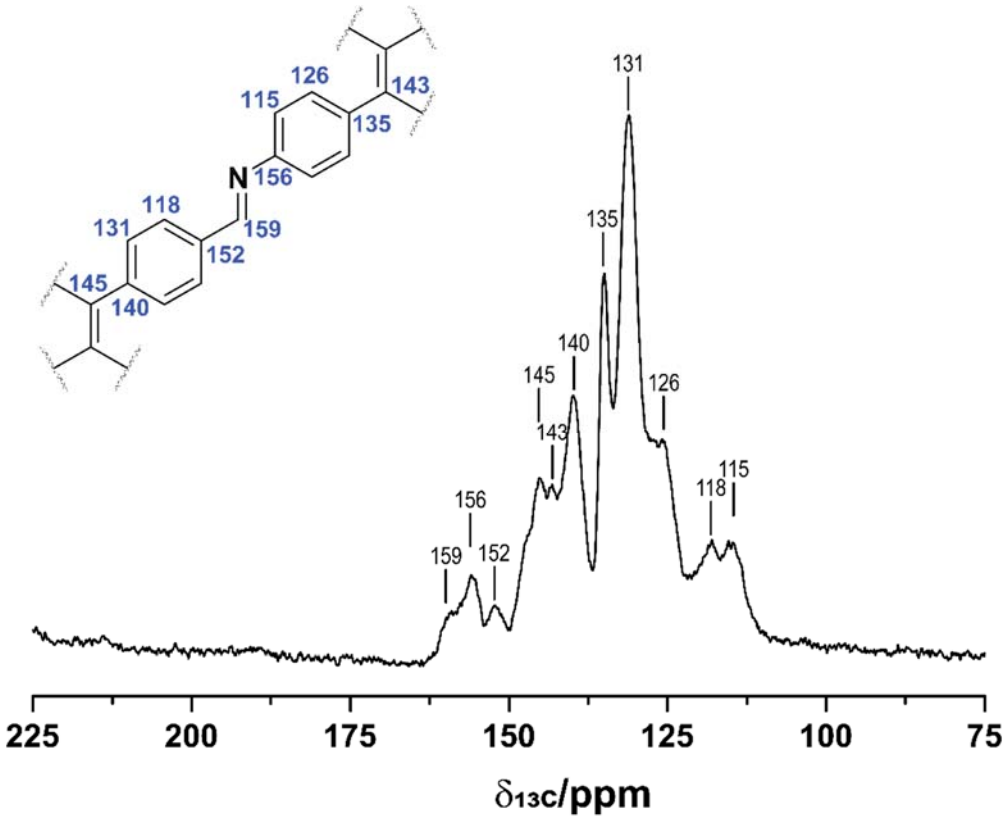

Figure S15. Solid-state ^{13}C CP/MAS NMR spectrum of TPE-COF-I. The assignments of ^{13}C chemical shifts were indicated in the chemical structure.

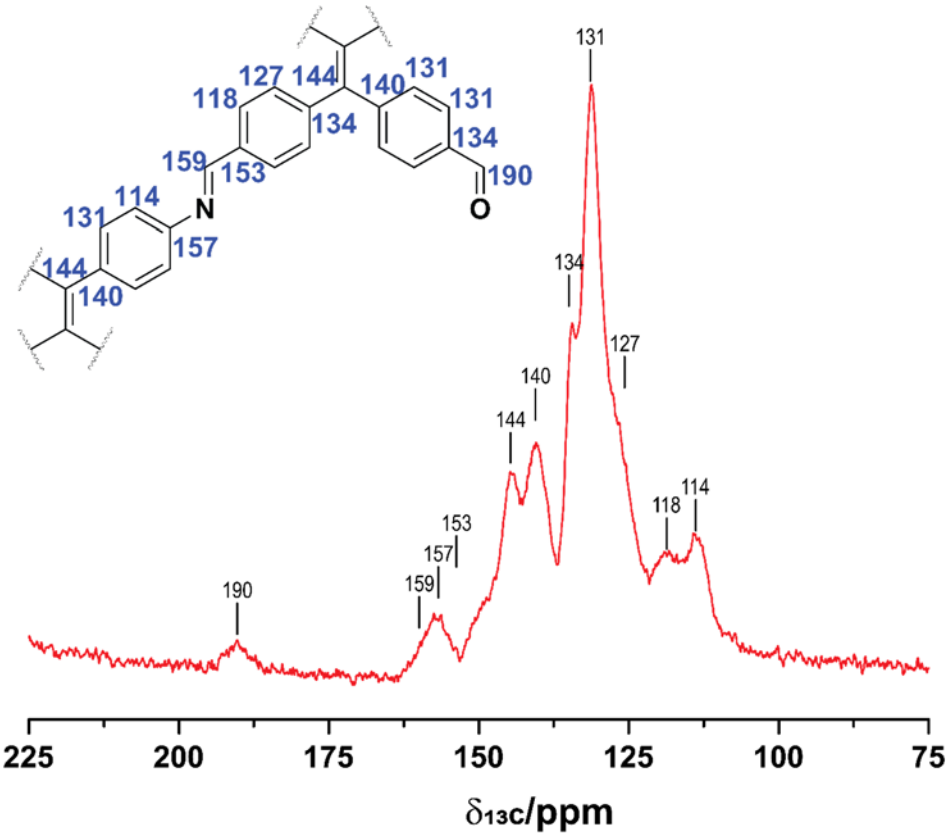

Figure S16. Solid-state ^{13}C CP/MAS NMR spectrum of TPE-COF-II. The assignments of ^{13}C chemical shifts were indicated in the chemical structure.

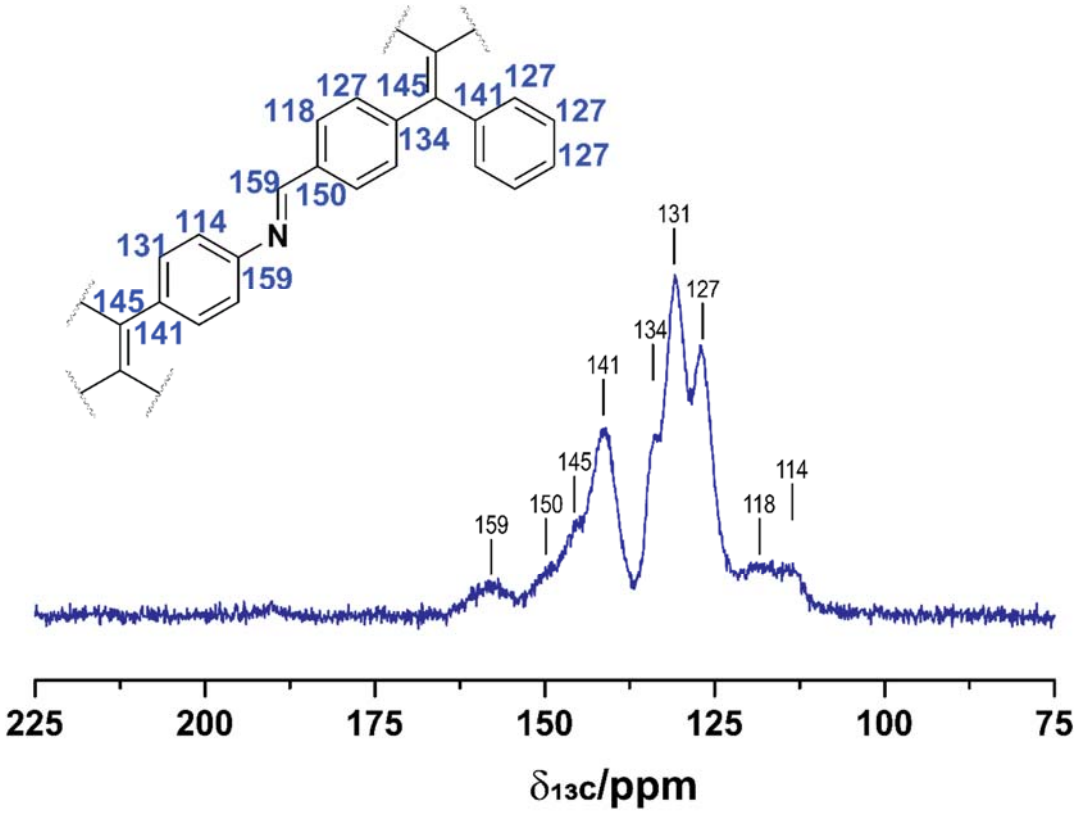

Figure S17. Solid-state ^{13}C CP/MAS NMR spectrum of TPE-COF-III. The assignments of ^{13}C chemical shifts were indicated in the chemical structure.

V. FT-IR spectra of monomer, model compounds and TPE-COFs

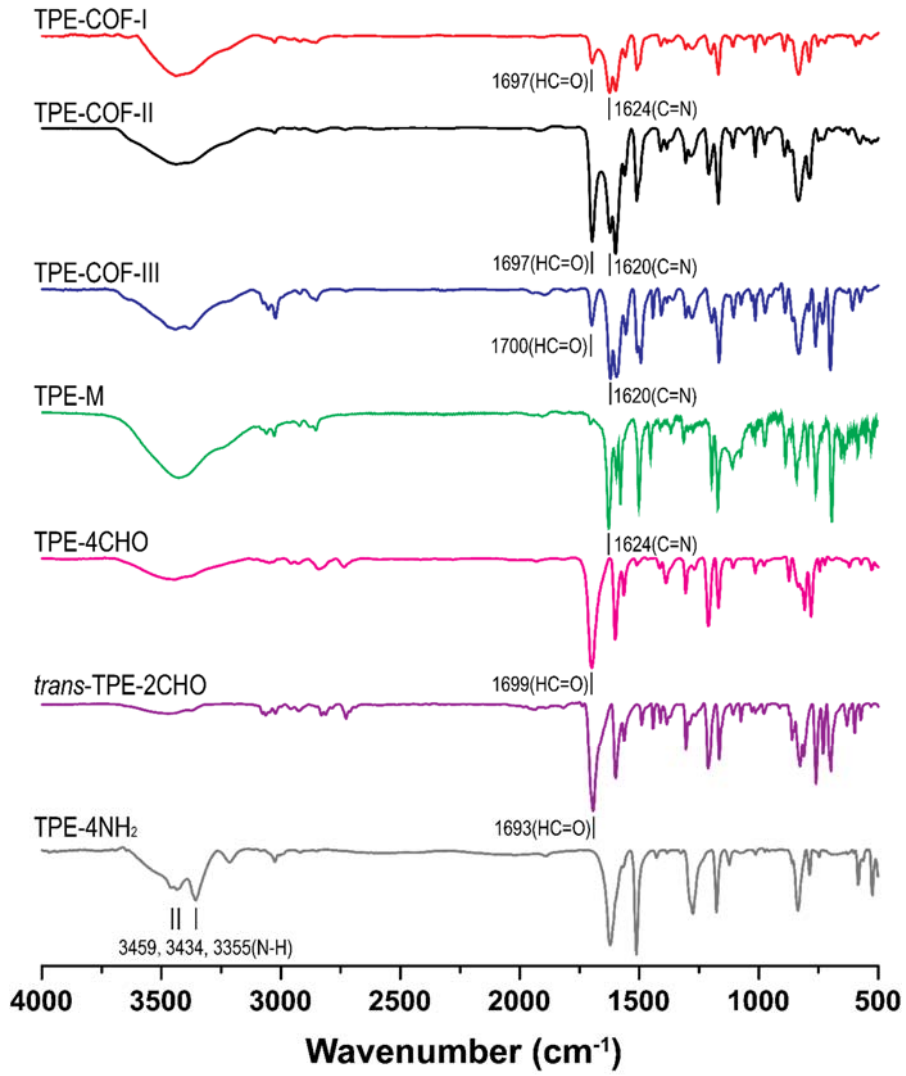

Figure S18. FT-IR spectra of TPE-COF-I (red), TPE-COF-II (black), TPE-COF-III (blue), model compound TPE-M (green), monomer TPE-4CHO (pink), *trans*-TPE-4CHO (purple) and TPE-4NH_2 (grey). The FT-IR spectra of TPE-COFs (blue) shows a –C=N– stretch at 1620-1624 cm^{-1}, indicating the successful formation of imine bonds. The bands at 1697 and 1700 cm^{-1} of TPE-COF-I and TPE-COF-III correspond to the terminal aldehyde and amino groups at the edges of TPE-COFs, while much stronger band at 1697 cm^{-1} of TPE-COF-II indicating the more aldehyde group existing in the structure.

VI. Thermogravimetric analysis of TPE-COFs

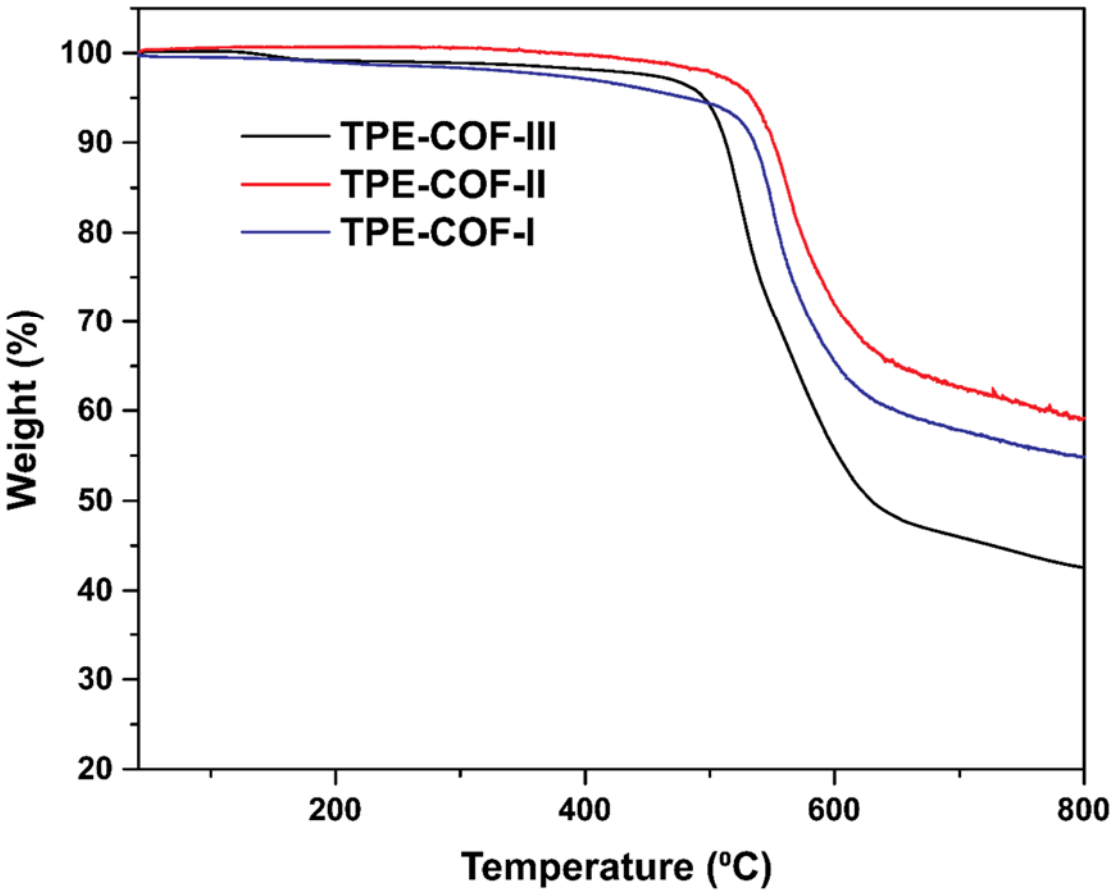

Figure S19. TGA data of TPE-COF-I (blue curve), TPE-COF-II (red curve), TPE-COF-III (black curve), all the TPE-COFs are thermally stable up to 450 °C.

VII. Gas sorption data of TPE-COFs

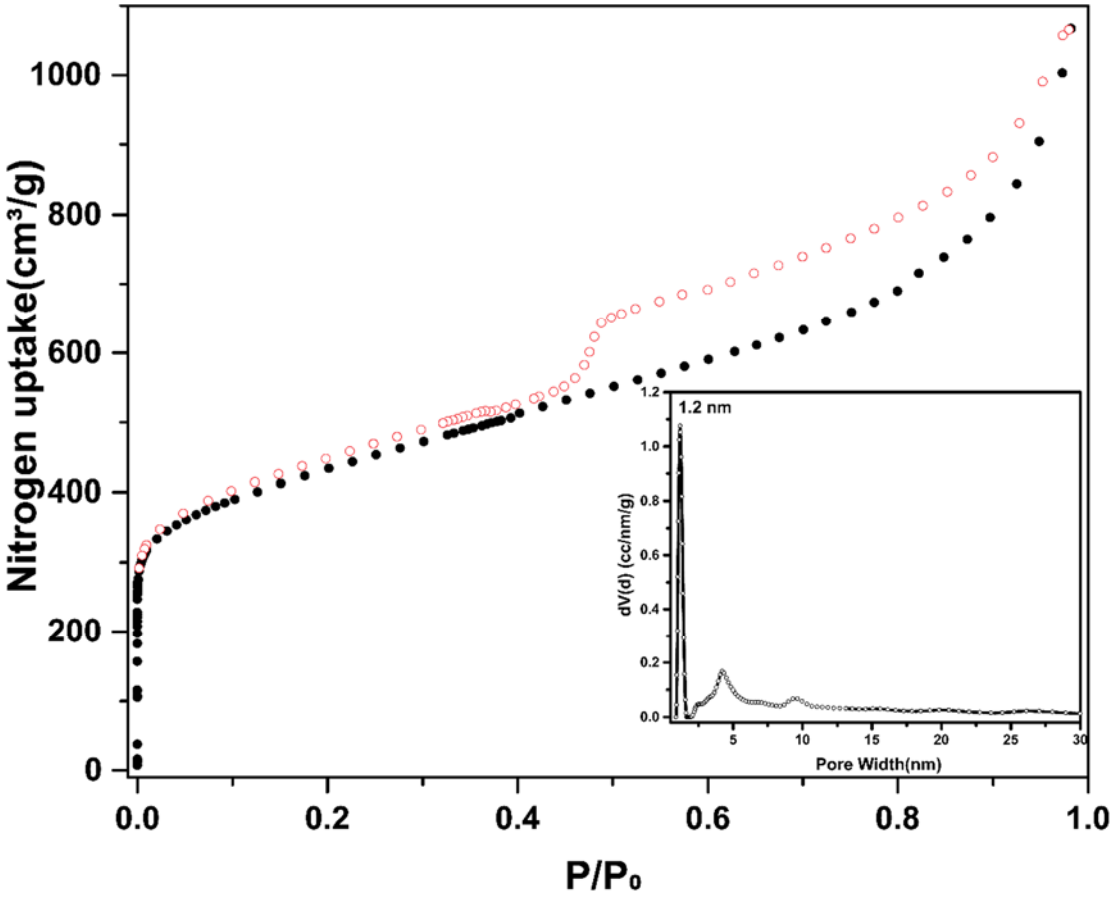

Figure S20. Nitrogen adsorption (filled symbols●) and desorption (empty symbols○) isotherms of TPE-COF-I, (inset) pore size distribution of TPE-COF-I. BET surface area = 1535 m^2/g, total pore volume = 1.65 (P/P_0 = 0.983), N_2 at 77 K on carbon (cylindr. pores, QSDFT adsorption branch).

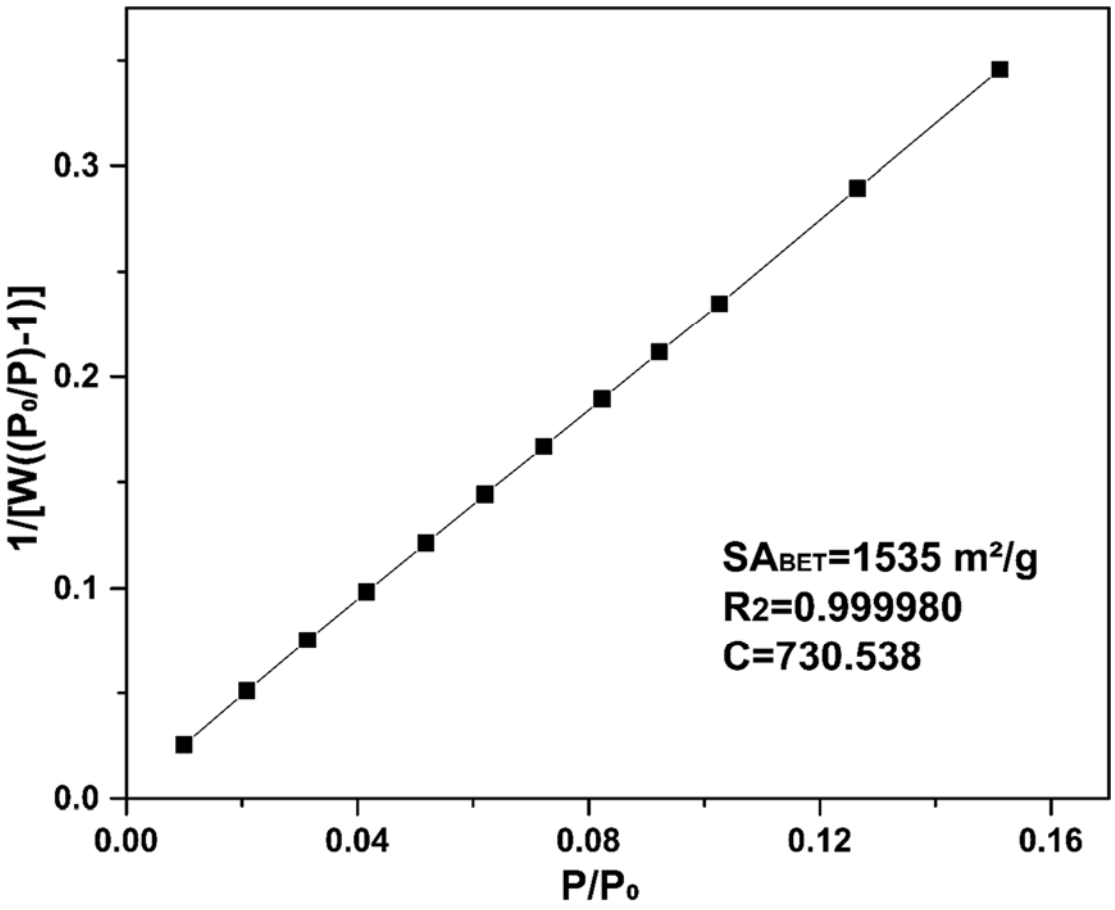

Figure S21. BET plot of TPE-COF-I calculated from N_2 adsorption isotherm at 77 K, with C value of 730.538.

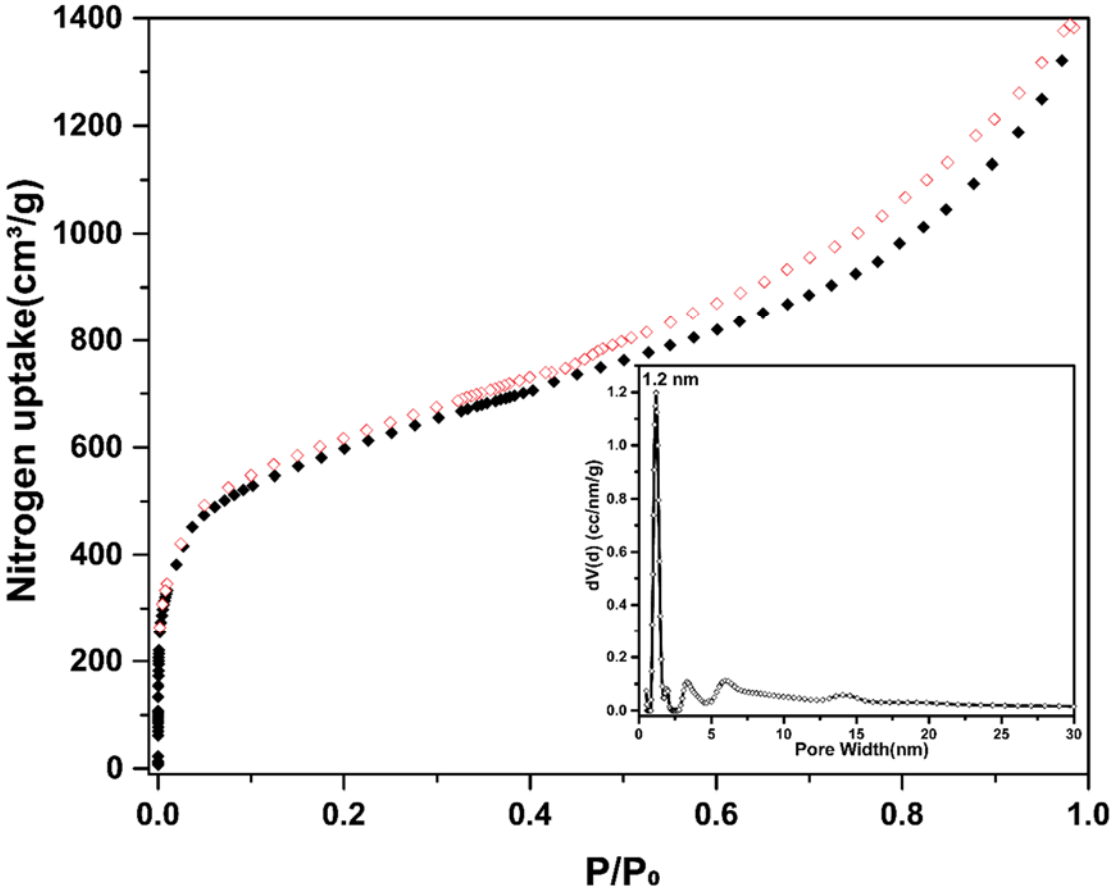

Figure S22. Nitrogen adsorption (filled symbols◆) and desorption (empty symbols◇) isotherms of TPE-COF-II, (inset) pore size distribution of TPE-COF-I, BET surface area = 2168 m^2/g, total pore volume = 2.14 (P/P_0 = 0.984), N_2 at 77 K on carbon (slit/cylindr. pores, QSDFT adsorption branch).

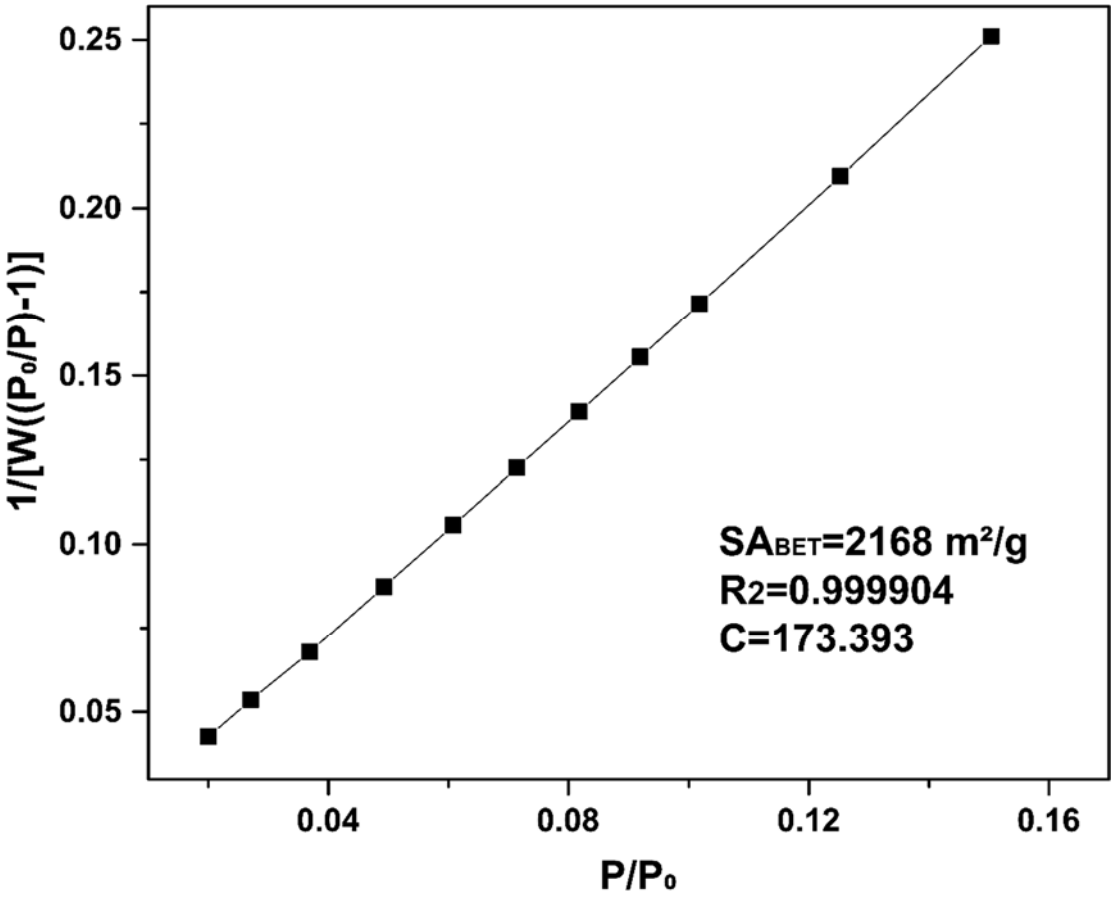

Figure S23. BET plot of TPE-COF-II calculated from N_2 adsorption isotherm at 77 K, with C value of 173.393.

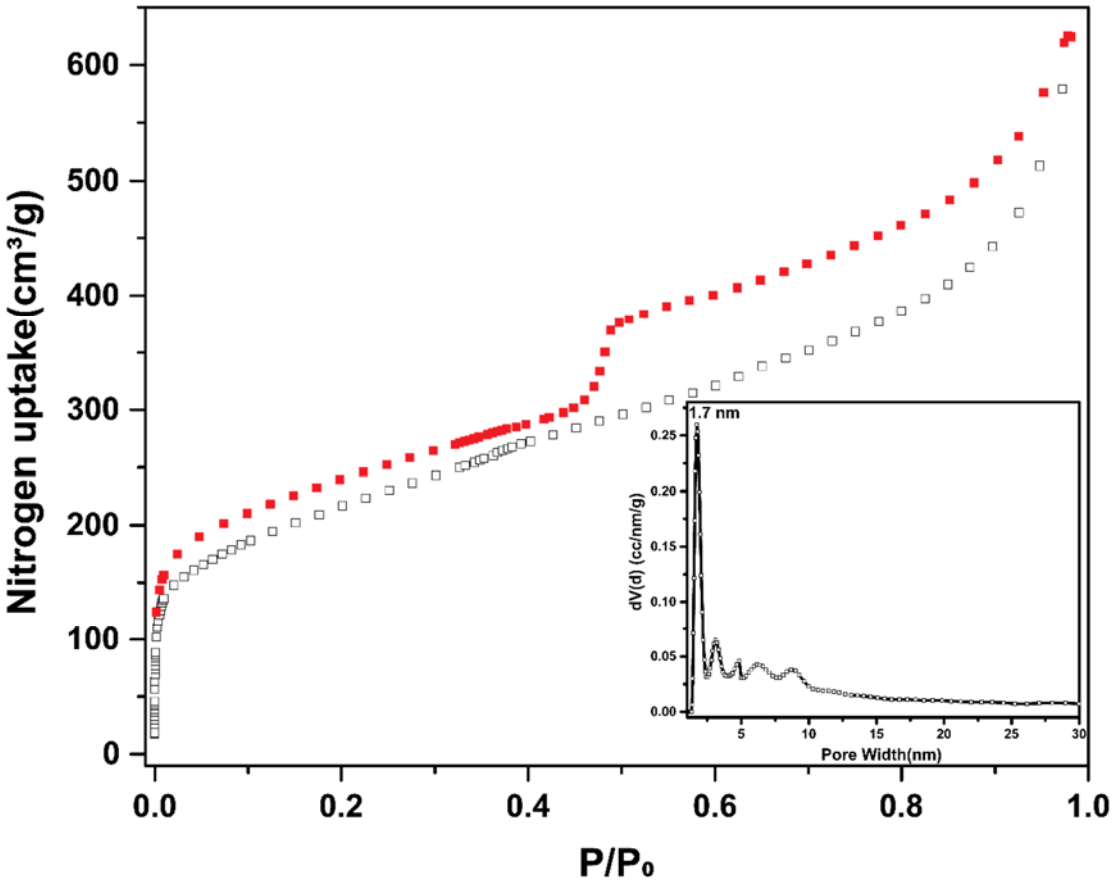

Figure S24. Nitrogen adsorption (filled symbols■) and desorption (empty symbols□) isotherms of TPE-COF-III, (inset) pore size distribution of TPE-COF-III. BET surface area = 774 m^2/g, total pore volume = 0.97 (P/P_0 = 0.982) N_2 at 77 K on carbon (cylindr./sphere pores, QSDFT adsorption branch).

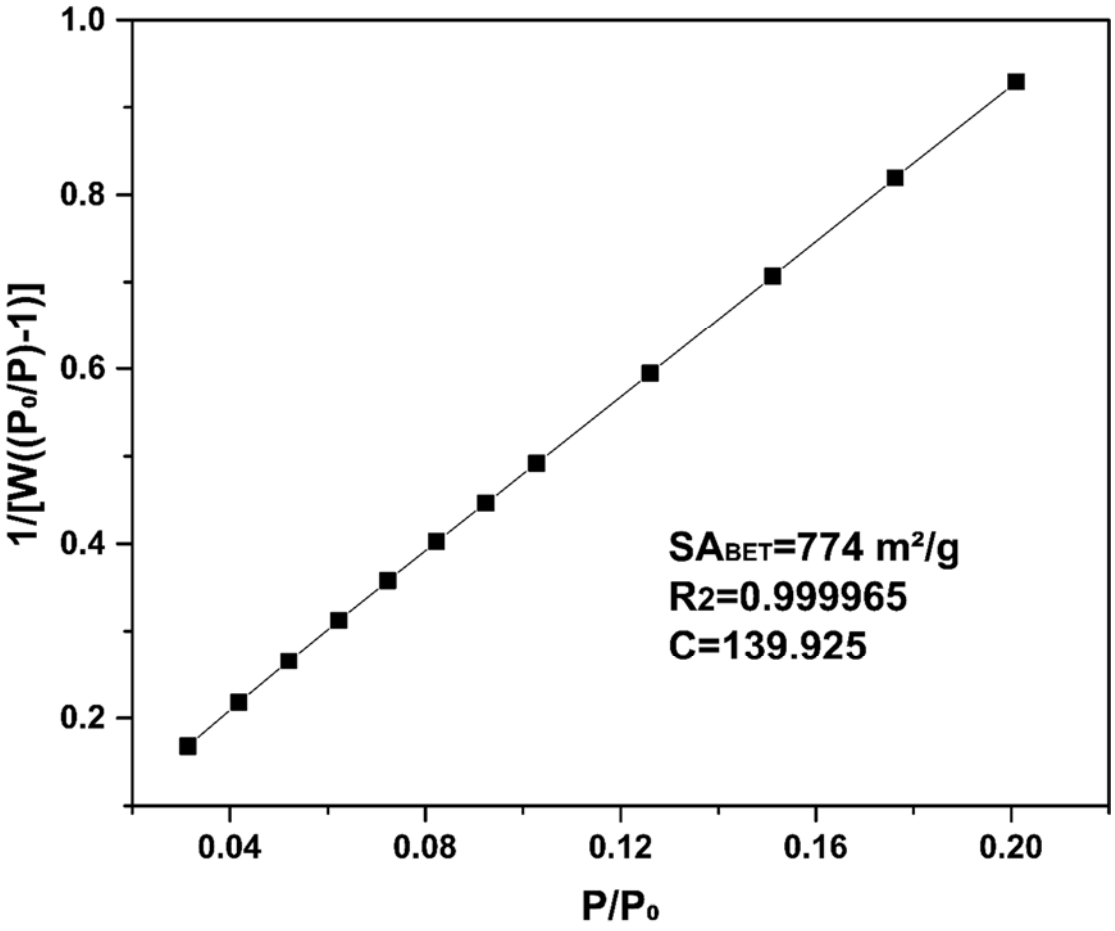

Figure S25. BET plot of TPE-COF-III calculated from N_2 adsorption isotherm at 77 K, with C value of 139.925.

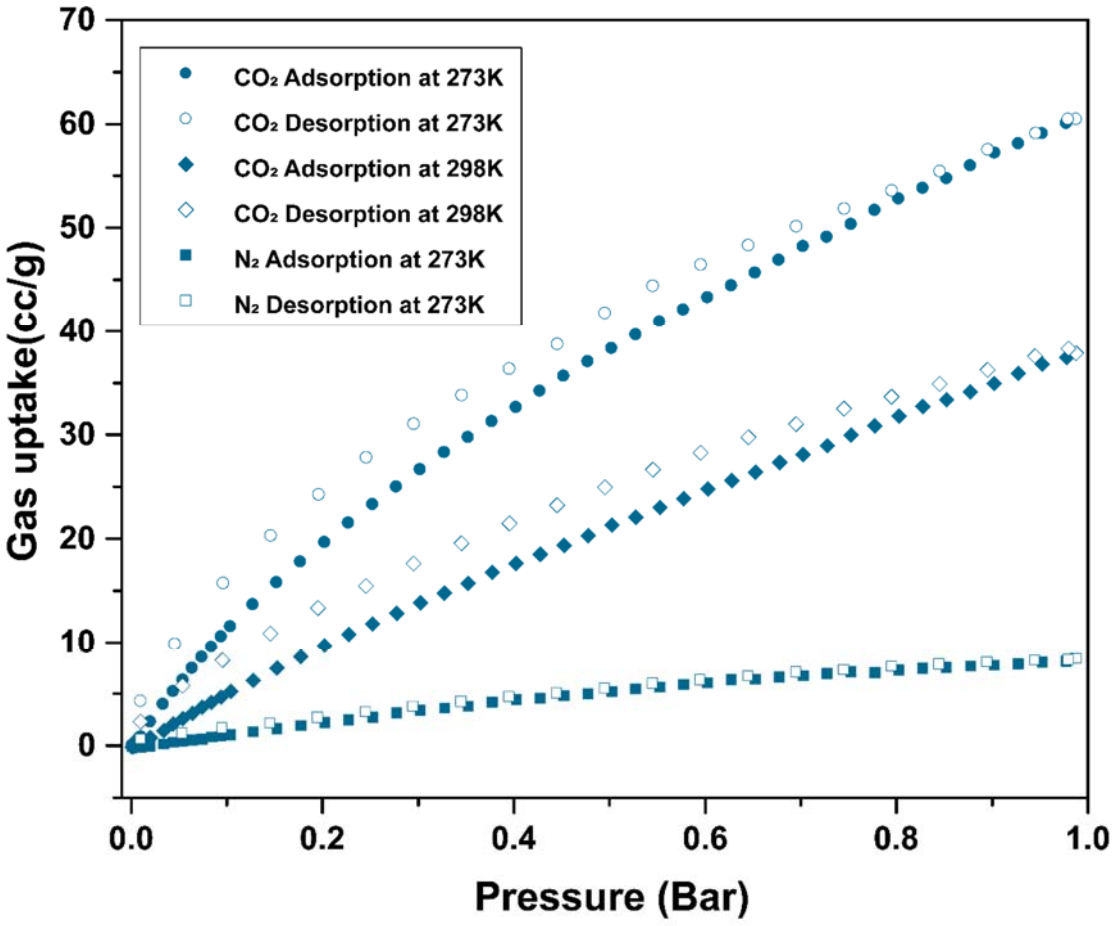

Figure S26. CO_2 adsorption isotherm of TPE-COF-I at 273 K(●), 298K (◆); N_2 adsorption isotherm of TPE-COF-I at 273 K(■)

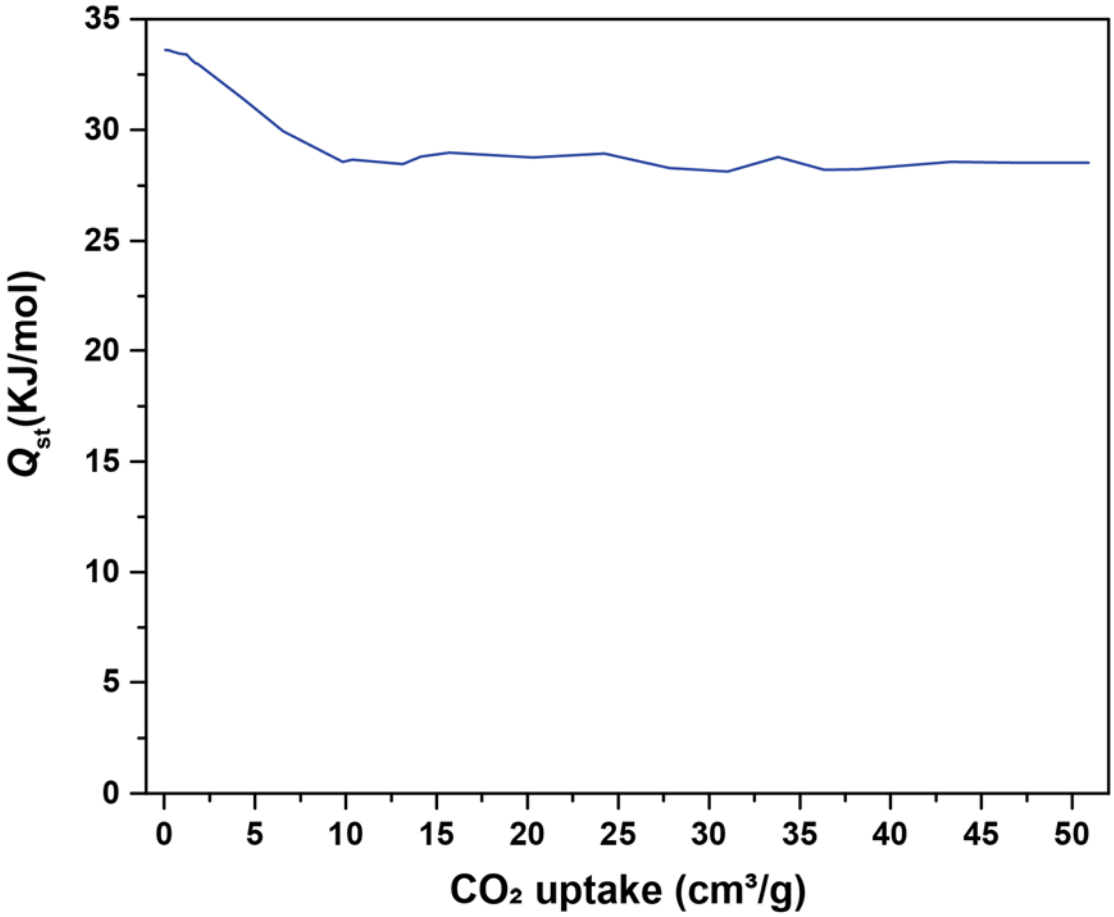

Figure S27. Isosteric heat of CO_2 adsorption for TPE-COF-I calculated from CO_2 adsorption isotherms at 273 and 298 K.

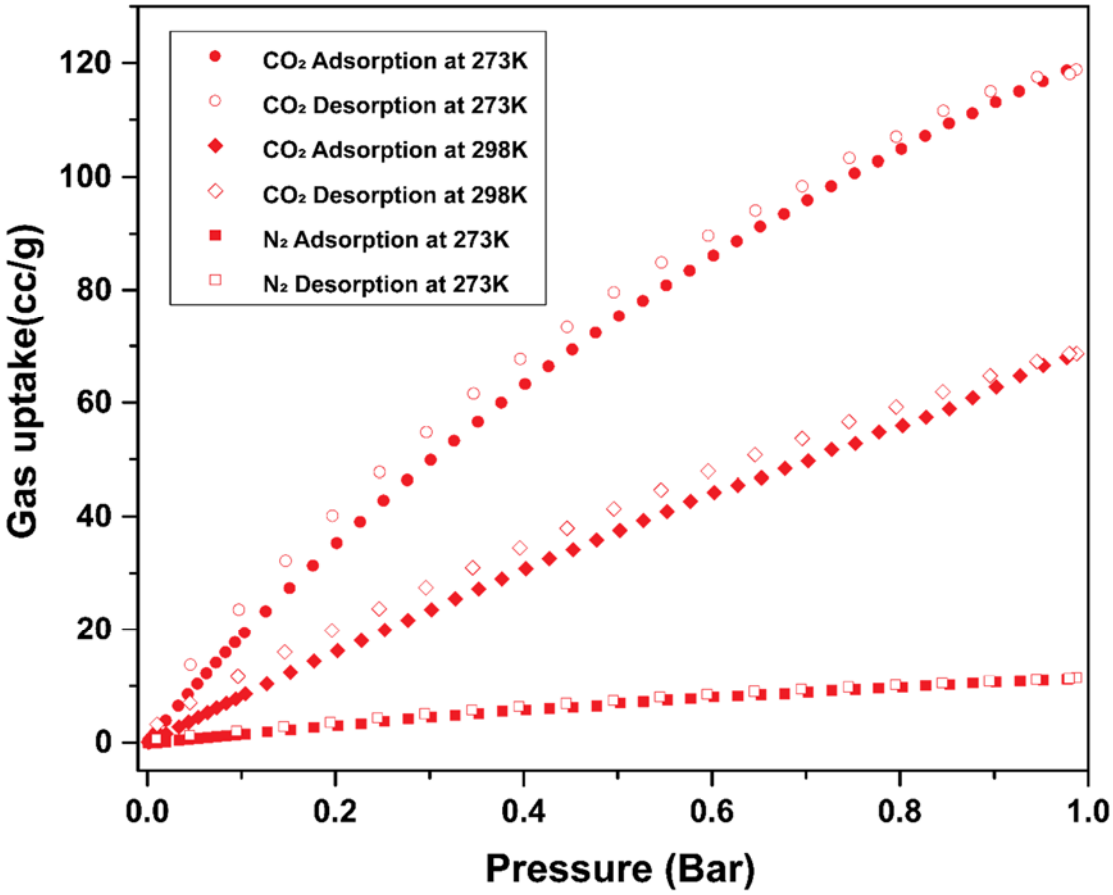

Figure S28. CO_2 adsorption isotherm of TPE-COF-II at 273 K(●), 298K (◆); N_2 adsorption isotherm of TPE-COF-II at 273 K(■)

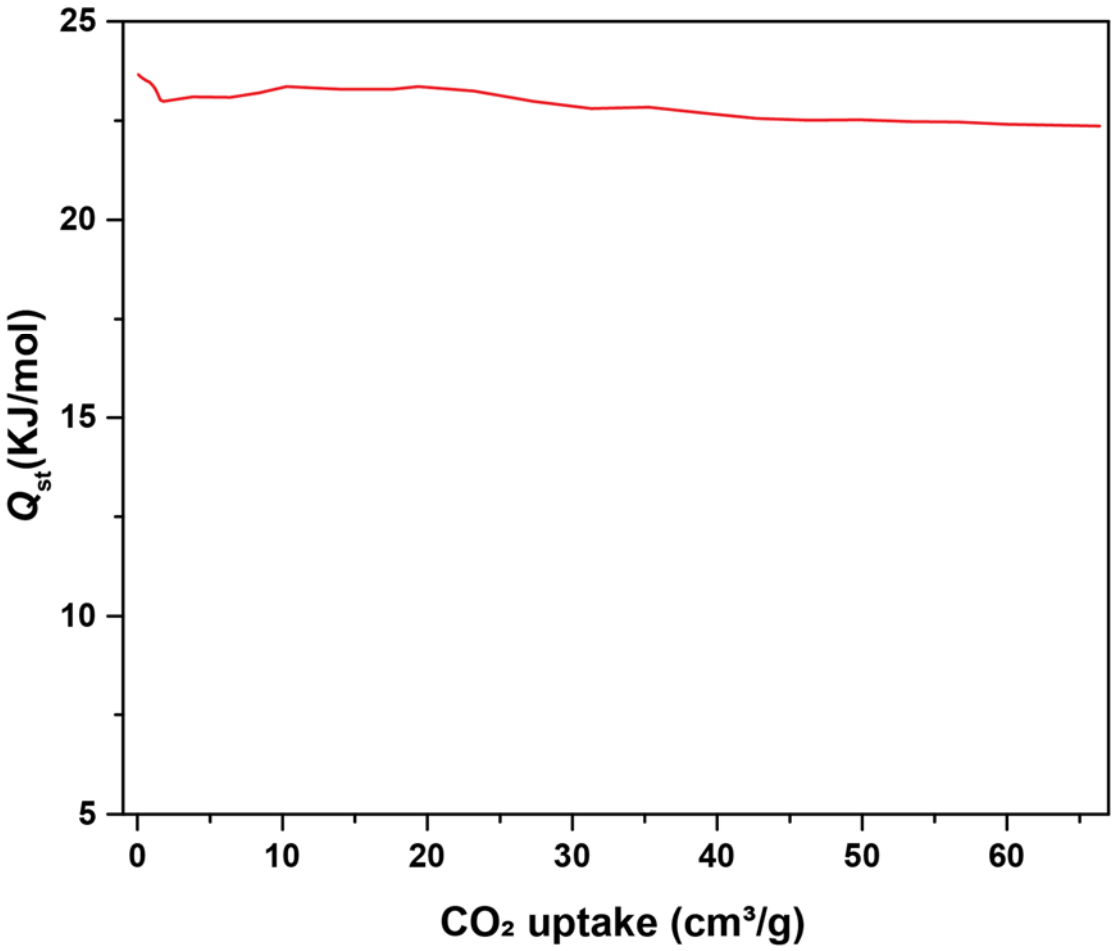

Figure S29. Isosteric heat of CO_2 adsorption for TPE-COF-II calculated from CO_2 adsorption isotherms at 273 and 298 K.

VIII. SEM and TEM image of TPE-COFs

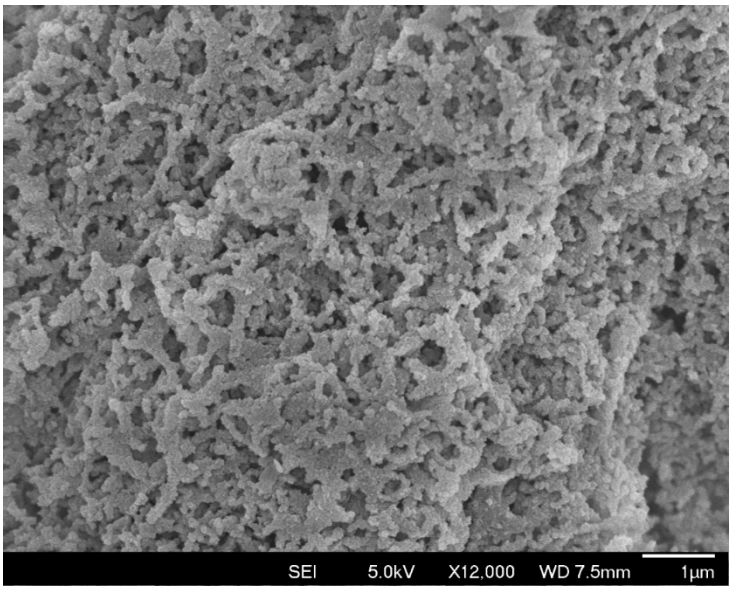

Figure S30. SEM image of TPE-COF-I. The image shows that TPE-COF-I adopts a coral-like morphology, which indicates its high crystallinity.

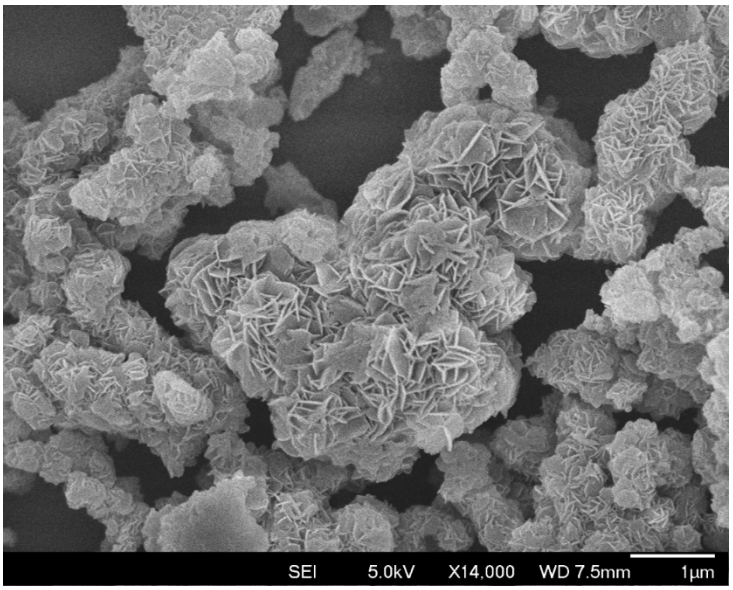

Figure S31. SEM image of TPE-COF-II. The image shows that TPE-COF-II adopts a sheet-like morphology, which indicates its high crystallinity.

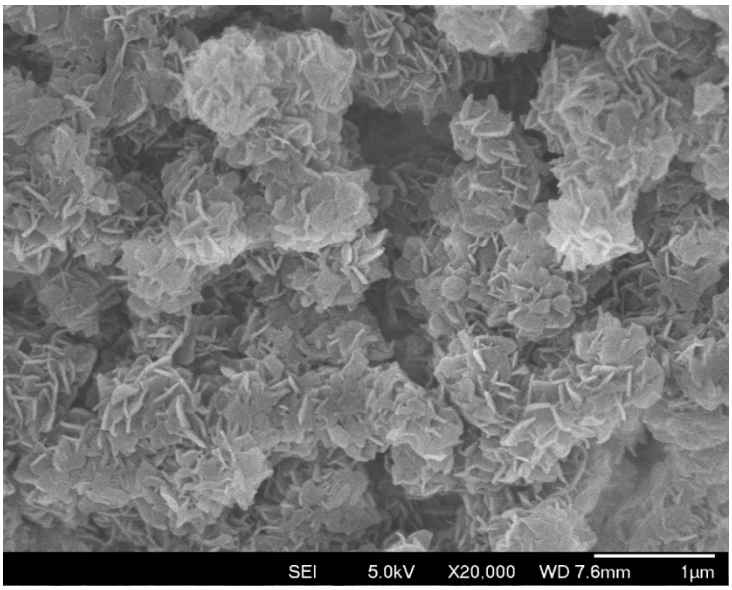

Figure S32. SEM image of TPE-COF-III. The image shows that TPE-COF-III adopts a sheet-like morphology, which indicates its high crystallinity.

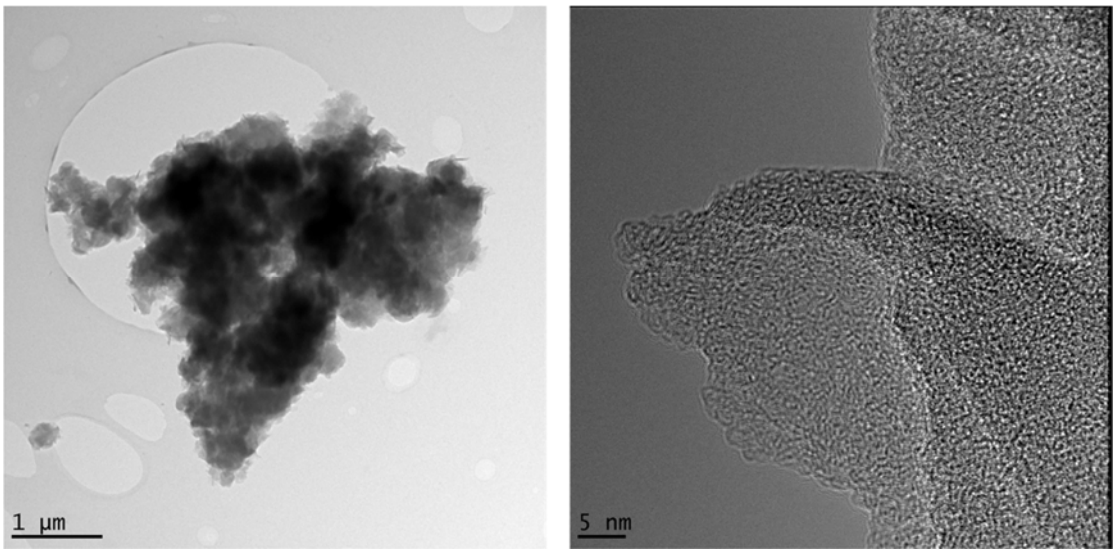

Figure S33. TEM image of TPE-COF-I, indicating the uniform porous structure and high crystallinity.

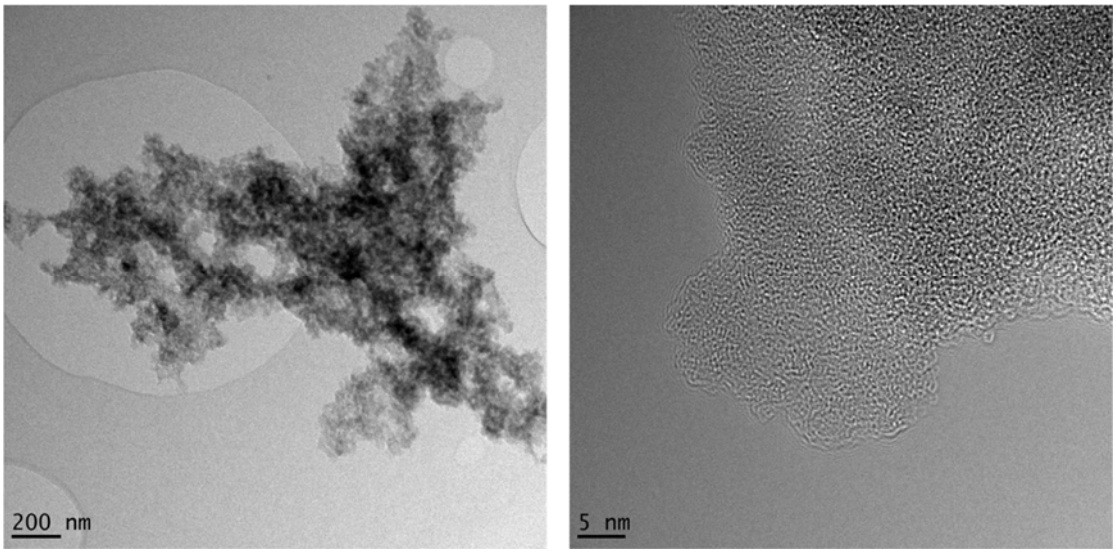

Figure S34. TEM image of TPE-COF-II, indicating the uniform porous structure and high crystallinity.

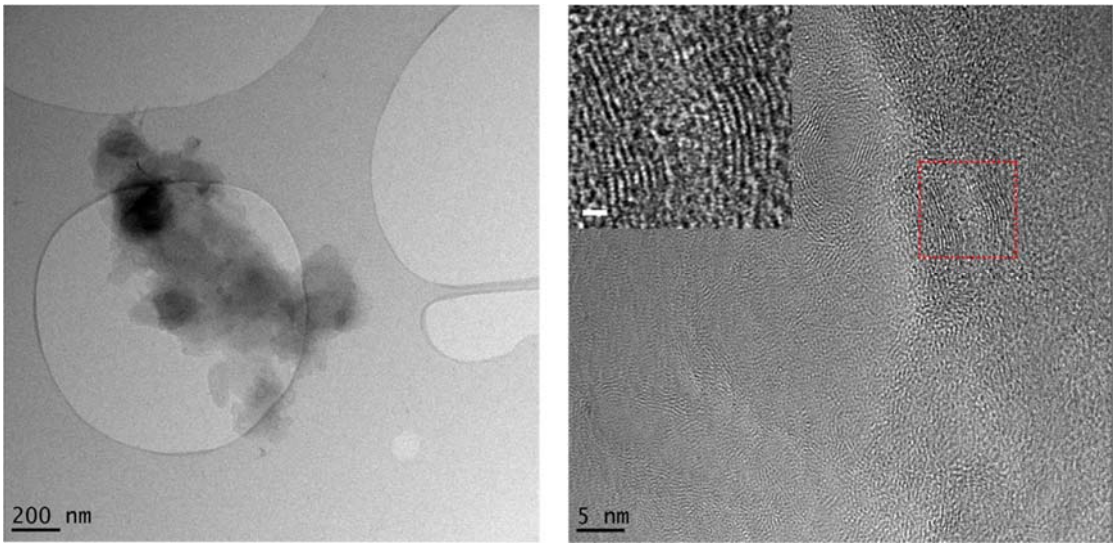

Figure S35. TEM image of TPE-COF-III, indicating the uniform porous structure and high crystallinity.

IX. Structure Modelling of TPE-COFs[4]

Table S2 Fractional atomic coordinates for the unit cell of TPE-COF-I with *PM* space group.

Space Group: monoclinic, *PM* (No. 6) a = 20.4043Å, b = 15.7014 Å, c = 5.1963 Å; $\alpha = \gamma = 90.0^{o}$, $\beta = 86.50^{o}$ wR_p = 2.75%, R_p = 2.09%			
Atom	x	y	z
C1	0.33965	0.85545	-0.00162
C2	0.3942	0.90576	-0.07263
C3	0.44925	0.85362	0.29458
C4	0.39484	0.80287	0.36534
C5	0.33955	0.8039	0.21926
N6	0.2842	0.24792	0.29847
C7	0.44887	0.09355	0.07768
C8	0.06686	0.59364	0.41356
C9	0.065	0.64617	0.19649
C10	0.11885	0.69711	0.12027
C11	0.1226	0.59459	0.55817
C12	0.175	0.30355	0.26117
C13	0.17665	0.35477	0.48158
C14	0.23089	0.24995	0.17508
C15	0.00808	0.54341	0.4981
H16	0.01933	0.64756	0.08067
H17	0.11707	0.73941	-0.05747
H18	0.12404	0.5539	0.73944
H19	0.22212	0.35516	0.59862
H20	0.29508	0.85631	-0.12363
H21	0.39443	0.94663	-0.25401
H22	0.49433	0.85217	0.41376
H23	0.3954	0.76034	0.54301
C24	0.83965	0.35545	-0.50162
C25	0.8942	0.40576	-0.57263
C26	0.94925	0.35362	-0.20542
C27	0.89484	0.30287	-0.13466
C28	0.83955	0.3039	-0.28074
C29	0.7842	0.74792	-0.20153
C30	0.94887	0.59355	-0.42232
C31	0.56686	0.09364	-0.08644
C32	0.565	0.14617	-0.30351
C33	0.61885	0.19711	-0.37973
C34	0.6226	0.09459	0.05817
C35	0.675	0.80355	-0.23883
C36	0.67665	0.85477	-0.01842
N37	0.73089	0.74995	-0.32492

C38	0.50808	0.04341	-0.0019
H39	0.51933	0.14756	-0.41933
H40	0.61707	0.23941	-0.55747
H41	0.62404	0.0539	0.23944
H42	0.72212	0.85516	0.09862
H43	0.79508	0.35631	-0.62363
H44	0.89443	0.44663	-0.75401
H45	0.99433	0.35217	-0.08624
H46	0.8954	0.26034	0.04301
H47	1.22669	0.20938	-1.00512
H48	0.78844	0.78857	-0.02153

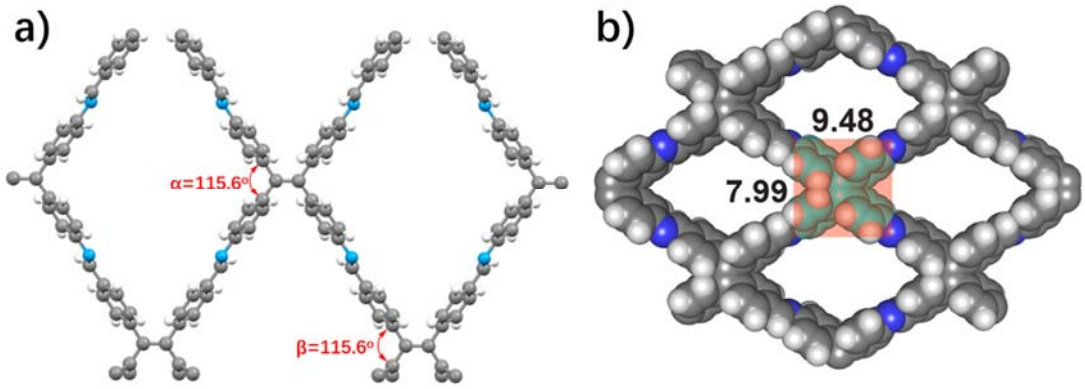

Figure S36. a) The bond angles of two *cis*-carbons in amine and aldehyde TPE building units (α = β = 115.6°), measured from simulated crystal structure in TPE-COF-I. b) The size of amine TPE building unit in the TPE-COF-I, 9.48 Å × 7.99Å.

Table S3 Fractional atomic coordinates for the unit cell of TPE-COF-II with *C2/m* space group.

Space Group: monoclinic, *C2/m* (No. 12) a = 26.4625 Å; b= 44.0191 Å; c = 5.6343 Å; $\alpha = \gamma = 90.0^{o}$, β =109.87^{o} wR_p = 2.91% ; R_p = 2.30%			
Atom	x	y	z
N1	0.34677	0.10834	0.31699
C2	0.35232	0.13465	0.22554
C3	0.32538	0.16088	0.29053
C4	0.1296	0.19594	0.62555
C5	0.17722	0.21157	0.66112
C6	0.18551	0.2271	0.46003
C7	0.14282	0.22994	0.23125
C8	0.0941	0.21514	0.19786
C9	0.45029	0.03357	0.40612
C10	0.41737	0.03686	0.5533
C11	0.37904	0.05978	0.50083
C12	0.37593	0.08121	0.31403
C13	0.40709	0.07746	0.15853
C14	0.44373	0.05357	0.20416
C15	0.08854	0.19665	0.39052
C16	0.30074	0.15781	0.47367
C17	0.27552	0.18234	0.53889
C18	0.27339	0.21065	0.42149
C19	0.29835	0.21375	0.23844
C20	0.32542	0.18925	0.17843
C21	0.25926	0.26444	0.52482
C22	0.04208	1.82354	0.34182
O23	0.54685	0.34791	0.44971
H24	0.37762	0.13696	0.09821
H25	0.12398	0.18253	0.7879
H26	0.20995	0.21185	0.85492
H27	0.14779	0.24431	0.0723
H28	0.05891	0.21809	0.01421
H29	0.42192	0.02068	0.71729
H30	0.35	0.06111	0.6106
H31	0.40237	0.09389	-0.00399
H32	0.4685	0.05038	0.07532
H33	0.3014	0.13497	0.57005
H34	0.25609	0.17971	0.68995
H35	0.2966	0.23639	0.13765
H36	0.34752	0.19238	0.03819
H37	0.00921	0.81028	0.38486
C38	0	0.48465	0.5

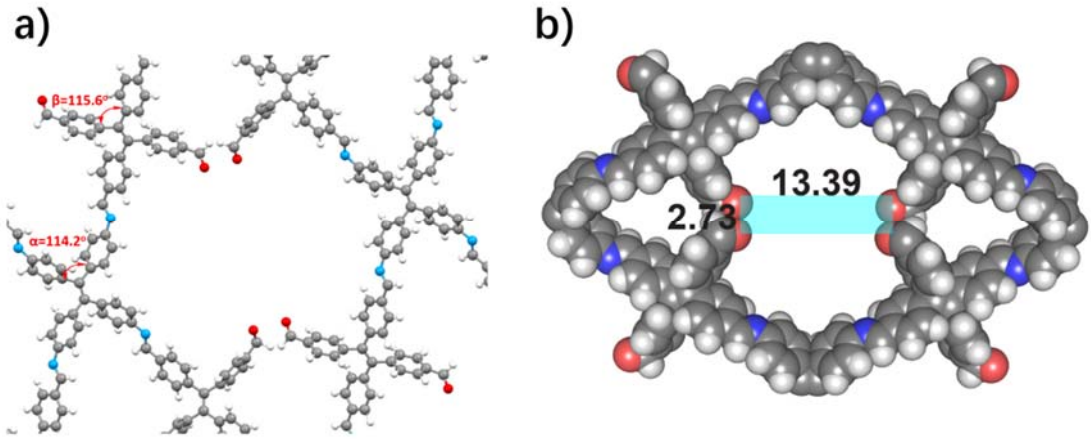

Figure S37. a) The bond angles of two *cis*-carbons in amine and aldehyde TPE building units were 114.2° and 115.6°, measured from simulated crystal structure in TPE-COF-II. b) The size of TPE building unit vacancy in the TPE-COF-II, 13.39 Å × 2.73 Å.

Table S4 Fractional atomic coordinates for the unit cell of TPE-COF-III with *C2/m* space group.

Space Group: monoclinic, *C2/m* (No. 12) a = 26.3252 Å; b= 44.5426 Å; c = 5.6472 Å; $\alpha = \gamma = 90.0^{o}$, β=110.95^{o} wR_p=4.41% ; R_p=3.55%			
Atom	x	y	z
N1	0.33816	0.10492	0.36046
C2	0.33337	0.12977	0.22982
C3	0.30347	0.15608	0.27611
C4	0.10164	0.22567	0.5709
C5	0.15653	0.22478	0.60591
C6	0.17607	0.23797	0.42685
C7	0.13981	0.25218	0.21383
C8	0.08498	0.25311	0.17972
H9	0.35475	0.13281	0.09891
H10	0.08687	0.21555	0.70976
H11	0.18368	0.2144	0.77511
H12	0.05733	0.26415	0.01501
C13	0.44996	0.03359	0.42426
C14	0.41827	0.0346	0.57861
C15	0.37843	0.05671	0.54052
C16	0.37175	0.07931	0.35718
C17	0.40202	0.07748	0.1944
C18	0.44073	0.05482	0.22854
C19	0.06588	0.2398	0.35785
C20	0.27652	0.15494	0.45207
C21	0.25264	0.1811	0.50735
C22	0.25583	0.20888	0.39039
C23	0.28001	0.20942	0.20431
C24	0.30448	0.18347	0.15119
H25	0.35508	0.05737	0.66509
H26	0.39776	0.09384	0.04622
H27	0.46563	0.05482	0.11071
H28	0.27495	0.13409	0.55127
H29	0.23323	0.17965	0.6472
H30	0.32498	0.18488	0.0148
C31	0.26568	0.26265	0.53778
H32	0.15385	0.7375	0.07413
H33	0.21956	0.7301	0.89769
H34	0.02343	1.75951	0.33115
H35	0.57484	0.98279	1.26361
C36	0	0.48461	0.5

Table S5. Fractional atomic coordinates for the unit cell of another possible TPE-COF-IV with *C2/m* space group, which simulated PXRD showed no agreement with experimental PXRD.

Space Group: monoclinic, *C2/m* (No. 12) a = 31.8035 Å; b= 40.7389 Å; c = 5.8314 Å; $\alpha = \gamma = 90.0^{o}$, β=92.9766^{o}			
Atom	x	y	z
N1	0.36118	0.10605	0.45023
C2	0.35009	0.127	0.29028
C3	0.31899	0.15285	0.33447
C4	0.13551	0.21485	0.7324
C5	0.17895	0.21768	0.71161
C6	0.19483	0.23093	0.51142
C7	0.16669	0.2416	0.33369
C8	0.12326	0.23888	0.35493
C9	0.46076	0.03623	0.47272
C10	0.43417	0.03978	0.65536
C11	0.40036	0.06165	0.63902
C12	0.39346	0.08141	0.44445
C13	0.42038	0.07813	0.26142
C14	0.45364	0.05567	0.27629
C15	0.10746	0.22545	0.55428
C16	0.29804	0.15368	0.54093
C17	0.27144	0.17982	0.58817
C18	0.26537	0.20556	0.43057
C19	0.28463	0.20397	0.21984
C20	0.31161	0.17801	0.17317
C21	0.25924	0.26503	0.5098
N22	0.06302	1.77724	0.57638
H23	0.3648	0.1271	0.12737
H24	0.12371	0.20461	0.88784
H25	0.19999	0.21027	0.85392
H26	0.17837	0.25225	0.17961
H27	0.10196	0.24731	0.21642
H28	0.44066	0.02691	0.81488
H29	0.3804	0.06425	0.78277
H30	0.41712	0.09337	0.11027
H31	0.47494	0.05435	0.13828
H32	0.30299	0.13458	0.66868
H33	0.25685	0.18036	0.75115
H34	0.27943	0.22329	0.09425
H35	0.32751	0.17798	0.01343
H36	0.44907	0.71298	0.27511
H37	0.45812	0.73056	0.5555
C38	0	0.48331	0.5

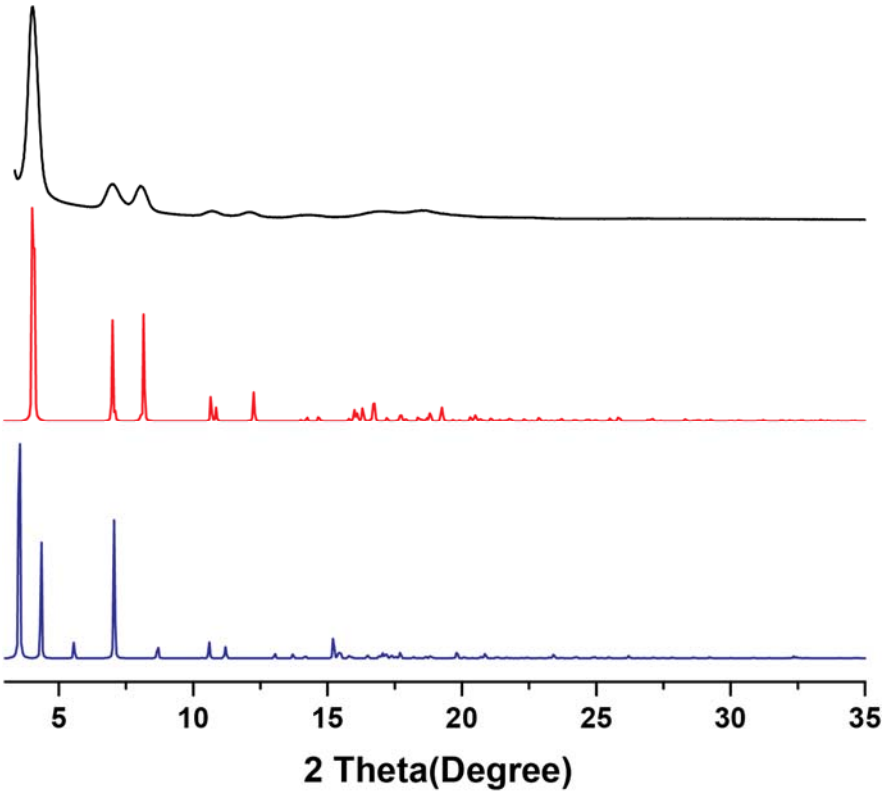

Figure S38. a) Experimental powder XRD patterns of TPE-COF-II (black); b) simulated powder XRD patterns of TPE-COF-II with eclipsed structure (red); c) simulated powder XRD patterns of TPE-COF-IV, another possible structure (blue). The simulated PXRD of TPE-COF-II showed very good agreement with experimental PXRD, while TPE-COF-IV showed no agreement with experimental PXRD.

Table S6. Summary of COFs materials for CO_2 capture (CO_2 capacities >100 cm^3g^{-1}) at low pressure (1.0 bar, 273K) reported in literatures.

COFs	SA_{BET} [$m^2\ g^{-1}$]	Pore Width (nm)	CO_2 capacities [$cm^3\ g^{-1}$]	Q_{st} [kJ mol^{-1}]
FCTF-1-600[5]	1535	0.46 and 0.54	124	32.0
TPE-COF-II	**2168**	**1.2**	**118**	**24.0**
TpPa-COF(MW)[6]	725	1.3	111	34.1
COF-JLU2[7]	415	0.96	110	31.0
FCTF-1[5]	662	0.46 and 0.55	105	35.0

XI. References:

(1) Reuter, S.; Bessinger, D.; Döblinger, M.; Hettstedt, C.; Karaghiosoff, K.; Herbert, S.; Knochel, P.; Clark, T.; Bein, T. *J. Am. Chem. Soc.* **2016**, 138, 16703.

(2) Ascherl, L.; Sick, T.; Margraf, J. T.; Lapidus, S. H.; Calik, M.; Hettstedt, C.; Karaghiosoff, K.; Döblinger, M.; Clark, T.; Chapman, K. W.; Auras, F.; Bein, T. *Nat. Chem.* **2016**, 8, 310.

(3) Bai, W.; Wang, Z.; Tong, J.; Mei, J.; Qin, A.; Sun, Z. J.; Tang, B. Z. *Chem. Commun.* **2015**, 51, 1089.

(4) Dassault Systèmes BIOVIA, Materials Studio, Version 2016, San Diego: Dassault Systèmes, 2017

(5) Zhao, Y.; Yao, K. X.; Teng, B.; Zhang, T.; Han, Y. *Energy Environ. Sci.* **2013**, 6, 3684.

(6) Wei, H.; Chai, S.; Hu, N.; Yang, Z.; Wei, L.; Wang, L. *Chem. Commun.* **2015**, 51, 12178.

(7) Li, Z.; Zhi, Y.; Feng, X.; Ding, X.; Zou, Y.; Liu, X.; Mu, Y. *Chem. Eur. J.* **2015**, 21, 12079.